Measurement and Modelling of Evapotranspiration

Magdalena Uber

September 15, 2016

Contents

Glossary 4

1 Measurement methods 8

1.1 Measurement of evaporation 8
1.1.1 Evaporation pans 8
1.1.2 Other evaporimeters 9
1.1.3 Micro-lysimeter 9
1.1.4 Soil heat pulse method 9
1.1.5 Measurement chambers 10
1.1.6 Micro Bowen ratio energy balance and eddy correlation methods 10
1.2 Measurement of interception 10
1.3 Measurement of transpiration 10
1.3.1 Porometers: measurement of gas exchange 10
1.3.2 Sap flow measurements 11
1.3.3 Measurement chambers 11
1.3.4 Biomass - transpiration relationship 12
1.4 Measurement of evapotranspiration 12
1.4.1 Lysimeter 12
1.4.2 Measurement chambers 13
1.4.3 Soil moisture measurements 14
1.4.4 Meterological measurements 15
1.4.5 Eddy-correlation measurements 15
1.4.6 Scintillometer measurements 17
1.4.7 Bowen Ratio 17
1.4.8 Isotopic compounds 18

2 Remote sensing 19

3 Calculation approaches 19

3.1 Water budget methods 20
3.2 Mass-transfer methods 20
3.3 Energy balance methods 21
3.4 Combinational methods: 22
3.4.1 Penmen 22
3.4.2 Priestley-Taylor 22
3.4.3 Penmen-Monteith 23
3.4.4 Schymanski and Or (2016) 26
3.5 Radiation-based methods 26
3.5.1 Turc's formula 26
3.5.2 Turc-Ivanov 26
3.5.3 Makkink 27
3.5.4 Jensen-Haise 27
3.5.5 Hargreaves 27
3.5.6 Doorenbos and Pruitt 27
3.5.7 McGuinnes and Bordne 27
3.5.8 Abtew 28
3.5.9 Priestley-Taylor 28

3.6 Temperature-based methods 28
3.6.1 Thornthwaite 28
3.6.2 Linacre 28
3.6.3 Blaney and Criddle 29
3.6.4 Kharrufa 29
3.6.5 Haude 29
3.6.6 Oudin 29
3.6.7 Others 29
3.7 Reference evapotranspiration 30
3.8 Others 31
3.8.1 Methods developed for remotely sensed data 31
3.8.2 Rutter 32
3.8.3 Numerical models 32

4 Water limitation **32**

5 Resistances **32**
5.1 Surface resistances 32
5.1.1 Single surface resistance 33
5.1.2 Canopy resistance or bulk stomatal resistance 34
5.1.3 Stomatal resistance 34
5.1.4 Architectural resistance 37
5.1.5 Surface resistance of (bare) soil 37
5.2 Aerodynamic resistance 39
5.2.1 Single aerodynamic resistance r_a 39
5.2.2 Above the canopy r_a^a 40
5.2.3 Between the canopy and mean surface flow height r_a^c . . 41
5.2.4 Between the soil surface and mean surface flow height r_a^s . 41

6 Arid and semi-arid regions **42**

Glossary

γ	psychromatic constant
$\delta\theta$	soil water deficit
Δ	rate of change saturated vapor pressure
ΔS	soil moisture storage change
ϵ_l	long wave emmissivity of the leaf surface
θ	soil moisture
θ_{fc}	soil moisture at field capacity
θ_{res}	residual soil moisture
θ_{wilt}	soil moisture at wilting point
λ	latent heat of vaporization $[cal\, g^{-1}]$
ρ	density of the air
σ_b	shielding factor
π_g	osmotic pressure of the guard cells of stomata
ϕ_M	atmospheric diabatic correction factor
ϕ_M	atmospheric diabatic correction factor for heat
ψ_g	water potential of the guard cells of stomata
ψ_h	stability correction function for sensible heat flux
ψ_m	stability correction function for momentum flux
ψ_l	leaf water potential
ψ_{pd}	pre-dawn leaf water potential
ψ_s	soil water potential
ω	monthly factor (Turc's formula)

a_t	coefficient for thermal expansion in air
A'	energy available for evaporation from the free water surface
A_{max}	maximum photosynthesis rate where CO_2 is not limited
A_{net}	net photosynthesis rate
ABA	abscisic acid
Bo	Bowen ratio
c_H	sensible heat transfer coefficient
C_d	parameter of the simplified Penman-Monteith equation FAO56-PM
C_n	parameter of the simplified Penman-Monteith equation FAO56-PM
C_p	specific heat of air
C_pl	plant coefficient of the Shuttleworth & Wallace model
C_s	soil coefficient of the Shuttleworth & Wallace model
C_w	water holding capacity
d	displacement height
d_l	duration of avarage monthly daylight
D	water vapor pressure deficit
D_h	diffusivity of heat
Dr	drainage
e	water vapor pressure
e_s	water vapor pressure at saturation
E	evaporation
ET	evapotranspiration
ET_0	reference evapotranspiration
ET_{act}	actual evapotranspiration
ET_{pot}	potential evapotranspiration
EVI	enhanced vegetation index
f_{BC}	proportionality factor of the Blaney & Criddle formula
f_c	fractinal vegetative cover
f_H	proportionality factor of the Haude formula
f_w	relatice surface wetness
F	fetch length
F_c	field capacity
FDR	frequency domain reflectancy
g	gravitational acceleration
g_s	stomatal conductance
G	ground heat flux
h_c	canopy height
h_v	surface vapor transfer coefficient
H	sensible heat flux
I	interception
I_h	heat index in THornthwaite's equation
Ir	irrigation
k	von Karman's constant ($= 0.41$)
K	correction coefficient for evaporation pans or evaporimeter
K_c	crop coefficient
K_h	eddy diffusion coefficient at the top of the canopy

K_r	crop specific root coefficient
K_x	xylem hydraulic conductivity
$K(z)$	eddy diffusion coefficient at height z
L	Monin-Obukhov length
LAI	leaf area index
M	molecular weight of air
M_v	molecular weight of water
MOST	Monin-Obukhov Similarity Theory
n	eddy diffusivity decay constant
N	number of days in a given month
NDVI	normalized difference vegetation index
p	percentage of daytime hours of total time
P	precipitation
P_{wa}	vapor pressure in the atmosphere
P_{was}	saturation vapor pressure at air temperature
$Perc.$	pecolation
q	specific humidity
q_r	relative humidity
Q	discharge
r	radius
r^*	critical resistance
r_a	aerodynamic resistance
r_a^a	aerodynamic resistance above the canopy
r_a^c	aerodynamic resistance between the canopy and mean surface flow height
r_a^s	aerodynamic resistance between the soil and mean surface flow height
r_{ah}	aerodynamic resistance to heat transfer
r_b	mean boundary layer resistance
r_s	surface resistance
r_s^c	canopy resistance / bulk stomatal resistance
r_s^{min}	minimum canopy resistance
r_s^s	surface resistance of bare soil
r_s^{st}	stomatal resistance
R	ideal gas constant
R^2	coefficient of determination
R_e	extraterrestrial radiation
R_g	incident solar radiation
R_n	net radiation
R_s	short wave radiation
RMSE	root mean square error
Ro	runoff
RWS	radio wave scintillometer
S	available soil water
SEE	soil evaporative efficiency
SF	stemflow
T	temperature
T_a	air temperature

T_d	dew point
T_l	leaf temperature
T_m	mean (monthly) temperature
T_{ref}	optimum T for photosynthesis
T_s	surface temperature
TDR	temperature domain reflectancy
TF	throughfall
TIR	thermal infrared radiation
Tr	transpiration
u	windspeed
u_*	friction velocity
u_h	wind speed at the top of the canopy
$u(z)$	windspeed at height z
v	kinematic viscosity
w	representative leaf width
W	upward water transfer from the water table
z	height
z_{0h}	roughness height for sensible heat flux
z_{0m}	roughness height for momentum
z_{0v}	roughness heitht for water vapor transfer

Table 1: Summary of the advantages and disadvantages of several evapotranspiration measurement methods from Rana and Katerji (2000).

Measurement method	Advantages	Disadvantages
Soil water balance	Soil moisture simple to be evaluated with gravimetric method Not expensive if the gravimetric method is used	Large spatial variability Difficult to be applied when the drainage and capillary rising are important Difficult to measure soil moisture in cracked soils
Weighing lysimeter	Direct method	Fixed Difficult maintenance It could be not representative of the plot area Expensive
Energy balance/ Bowen ratio	Simple sensors to be installed Suitable also for tall crops It can be also used when the fetch is 20:1 Not very expensive if psychrometers are used	Difficult to have correct measurement of the wet temperature if psychrometers are used The sensors need to be inverted to reduce bias Difficult maintenance
Aerodynamic	Simple sensors to be installed It does not need humidity measurements Not very expensive	It needs to be corrected for the stability Not suitable for tall crops
Eddy covariance	Direct method with fast hygrometer	Delicate sensors Difficult software for data acquisition Hygrometer very delicate expensive
Sap flow	Suitable for small plots It takes into account the variability among plants	Difficult scaling-up The gauges need to be deplaced every 1–2 weeks The soil evaporation is neglected
Chambers method	Suitable for small plots It can be used also for detecting emissions of different gases	It modifies the microclimate Difficult scaling-up

Table 2: Space and time scale of differnet methods to measure or model evapotranspiration, taken from Rana and Katerji (2000).

	Minute	Hour	Day	Month	Growth season	Year
Catchment				-----------Crop coefficient method-----------		
Uniform area	—Micrometeorological method--			------------Crop coefficient method----------		
				---------Soil water balance---------		
				------------Soil water balance with TDR------		
			------------Penman–Monteith model--------------			
Group of plants			-------Weighting lysimeter; chambers system--------			
			--------Sap flow--------			
Plant			--------Sap flow-------			

1 Measurement methods

Review over different measurement and calculation methods with regard to the Mediterranean region in Rana and Katerji 2000, see Table 1. Another good review of different measurement methods in Kool et al. (2014).

Different measurement (and calculation) approches cover different spatial and temporal scales (Table 2). Different methods are found to obtain systematic differences (e.g. Dugas et al. 1991 for measurement methods, Oudin et al. 2005 for calculation approaches).

1.1 Measurement of evaporation

1.1.1 Evaporation pans

Open tanks, filled with water, different surfaces and depths (e.g. Class A pan: 1.14 m^2, 0.2 m (Fig. 1), GGI 3000: 0.3 m^2, 0.685 m), measured pan evaporation equals neither potential nor actual evaporation, has to be corrected with a coeffiecient K which depends on climate, season and the type of pan. Used for estimating evaporation of lakes, dams etc., irrigated fields (Dyck and Peschke, 1995).

Figure 1: Class A evaporation pan with anemometer. http://www.sws.uiuc.edu/atmos/statecli/Instruments/panevap.jpg

Pan evaporation is also used as reference evaporation that is transformed to crop evaporation using crop coefficients (see sec. 3.7, Rana and Katerji 2000).

1.1.2 Other evaporimeters

Measurement of Evaporation from surfaces that are kept wet, e.g. filter paper (Piche-Atmometer) or ceramic disk (Czeratzki-Atmometer). Oasis effect has to be considered, so measurements also have to be corrected with a correction factor (Dyck and Peschke, 1995).

1.1.3 Micro-lysimeter

References: Shawcroft and Gardner (1983); Walker (1983); Daamen et al. (1993)

Small cylinder, usually 10 - 30 *cm* in depth and height, pushed into the soil surface, excavated, sealed at the bottom, weighed manually (usually daily) or continuously.
Advantages: simple, cheap, generally considered the most accurate method for measurement of soil evaporation. Disadvantages: time-consuming and low time resolution when weighed manually, unable to measure during rain or irrigation, limited representation of field conditions due to small sample size (Kool et al., 2014).

1.1.4 Soil heat pulse method

References: Heitman et al. (2008a,b)

Functioning: "The probe measures ambient temperature and temperature response curves to heat pulses, from which thermal properties can be derived. Evaporation can be estimated with heat pulse probes using an energy balance for a soil layer between two measurement depths by computing incoming and outgoing soil heat flux and heat storage. The energy that cannot be accounted for by the change in soil heat flux or heat storage, is attributed to latent heat flux" (Kool et al., 2014).

Advantages: continuous measurement of evaporation profiles below the surface, good results in field experiments. Disadvantages: Inability to measure E at the soil surface, during the first stage of evaporation (Kool et al., 2014).

1.1.5 Measurement chambers

See sec. 1.4.2. Applications in Musgrave and Moss (1961); Iritz et al. (1997); Raz-Yaseef et al. (2010, 2012); Domec et al. (2012)

1.1.6 Micro Bowen ratio energy balance and eddy correlation methods

Application of the Bowen ratio method (see sec. 1.4.7, Ashktorab et al. (1989); Holland et al. (2013)) or eddy correlation method (sec. 1.4.5 Wilson et al. (2001); Denmead et al. (1996)) on bare fields or under the canopy. Advantages: continuous measurement of relatively large surface areas. Disadvantages: high demand on measurement technique (measurement of temperature and humidity gradient at scales of few cm), methods still in developing stages, mostly applicable for tall canopies as measurement accuracy increases with height (Kool et al., 2014).

1.2 Measurement of interception

Measurement of precipitation (P), throughfall (TF) and stemflow (SF); P above the canopy or at a nearby clearing, TF and SF with randomly placed collectors, calculation of I with

$$I = P - TF - SF \tag{1}$$

1.3 Measurement of transpiration

Transpiration can be the dominant component of evapotranspiration (densely vegetated surfaces with a high extinction of incoming solar radiation, arid or semi-arid climates), can be an approximate estimate for evapotranspiration under such conditions (Dyck and Peschke, 1995). Whole-plant water use can be substantial: trees: 10 to $> 1000\ ld^{-1}$ (Wullschleger et al., 1998).

1.3.1 Porometers: measurement of gas exchange

Single leaves or twigs are inserted into a gas exchange chamber, measurement of gas concentrations (H_2O, CO_2) under controlled conditions of temperature, radiative intensity and air humidity.

Can also be used to determine stomatal conductance, e.g. in Lund and Soegaard (2003); Singer et al. (2010).

Disadvantage: microscale. (Dyck and Peschke, 1995).

Figure 2: Leaf porometer. http://www.hoskin.ca/catalog/images/Decagon%20Devices_E-240-40419.jpg

1.3.2 Sap flow measurements

Thermometric measurement of sap flow in xylem tissue based on conduction and convection of heat, three common methods: heat pulse, heat balance and constant heater methods (Burgess et al., 2001; Kool et al., 2014). Summary and literature in Kool et al. (2014)

Compensation heat pulse method (CHPM): heater is inserted into the xylem between two temperature sensors, e.g. 1st sensor - 0.5 *cm* - heater - 1.0 *cm* - 2nd sensor (Fig. 3). Heat pulse is considered to have reached the midpoint between the two sensors when both temperature sensors record the same temperature. Disadvantage: for low sap flow rates, heat dissipates before it reaches the midpoint, inverse sapflow direction cannot be traced, high sensitivity to inacuracies in the installation (Burgess et al., 2001).

Uncertainties in (semi-)arid regions because of the low transpiration rates (Rana and Katerji, 2000).

Other references: Kjelgaard et al. (1997); Grime and Sinclair (1999)

1.3.3 Measurement chambers

Measurement of transpiration in measurement chambers (see sec. 1.4.2) when plants are enclosed and separated from the soil surface. This disregards interaction between transpiration and evaporation and can cause errors in ET partitioning (Kool et al., 2014).

Figure 3: Sap flow measurement. http://au.ictinternational.com/products/sfm1/sfm1-sap-flow-meter/

1.3.4 Biomass - transpiration relationship

Estimation of transpiration from the linear relationship between relative total yield and relative accumulated transpiration. Advantage: robustnuss of the relation under varying environmental conditions. Disadvantage: destruction of the plants, inability to use small time steps (Kool et al., 2014).

1.4 Measurement of evapotranspiration

1.4.1 Lysimeter

Determination of the soil water balance of a weighed soil column, calculation of actual evapotranspiration:

$$ET = P - Perc. - \Delta S \quad [mm\, d^{-1}] \tag{2}$$

with P: precipitation, $Perc.$: percolation, ΔS: storage change.

Sources of error (Dyck and Peschke, 1995; Rana and Katerji, 2000):

- Formation of a capillary fringe above the bottom of the lysimeter, thus the lysimeter has to have a certain depth to ensure that this is not in the soil layer that impacts evapotranspiration.
- hydraulic contact with the surrounding soil.
- representativity of the vegetation on the lysimeter, thus the lysimeter has to have a certain diameter.
- vegetation growing over the rim of the lysimeter.
- In (semi-)arid regions cracks in the soil can cause periodic over- or under-estimation of ET.
- heating, wind shield and reflection of the metallic rim.

Disadvantages:

- expensive, few measurements possible
- only point measurement
- several sources of error (see above)

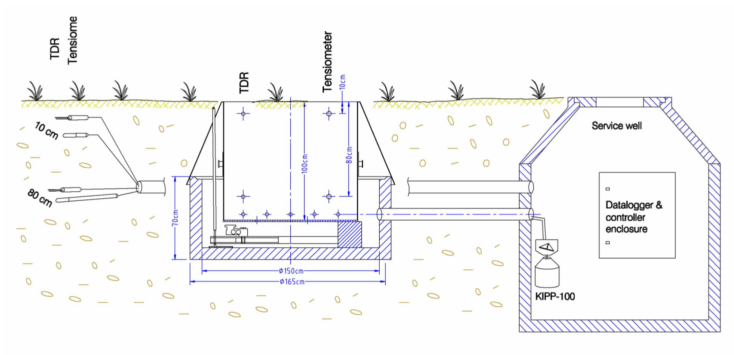

Figure 4: Sketch of a weighable lysimeter. http://www.ldd.go.th/18wcss/techprogram/P14033.HTM

1.4.2 Measurement chambers

Measurement of air humidity with a psychrometer before and after lowering of a cuboid or hemispherical plastic chamber on the plants / soil (Fig. 5). Other method: measurement of gas concentration changes. Dynamic chambers regulate climatic conditions in the chamber to represent conditions in the surrounding (Kool et al., 2014). Sizes of chambers can vary from small chambers including single plants to chambers of up to 100 m^3 (Denmead et al., 1993; Kool et al., 2014).

Accuracy of $\approx$ 10 % compared to lysimeter measurements (Reicosky et al., 1983). Comparison with Eddy-correlation and Bowen ratio measurements in arid Arizona in Dugas et al. (1991) gave a systematic overestimation by the chamber measurements compared to the other two methods, possible reasons: change of microclimate, edge effects, representativeness.

Main source of error: modification of the microclimate within the chamber which acts like a greenhouse: high transmissivity of shortwave radiation, low transmissivity of long wave radiation, altered energy balance, higher air temperature, different wind speed (Rana and Katerji, 2000). In irrigated field chamber measurement are subject to error due to advection of sensible heat from dry areas, measurements at the edge of a field not representative for the whole field (Dugas et al., 1991).

Only applicable on the microscale and at small timesteps, spatial and temporal extrapolation causes errors. very expensive equipment (55,000 USD, compared to 6,000 - 8,000 USD for Bowen ratio or EC systems, Dugas et al. 1991)

Other references: Musgrave and Moss (1961)

Figure 5: Measurement of soil evaporation and transpiration with a chamber system. Sources: https://faculty.unlv.edu/brian/pioneer/program_lang_files/image004.jpg and https://www.researchgate.net/profile/Robert_Lascano/publication/43278521/figure/fig1/AS:276816980922372@1443009720035/Fig-1-A-Wilted-cotton-plants-in-the-canopy-evapotranspiration-and-assimilation-CETA.png

1.4.3 Soil moisture measurements

Estimation of evapotranspiration from soil moisture measurements when horizontal water fluxes can be excluded and after percolation ended (soil moisture $\theta <$ field capacity F_c). Given these conditions soil moisture is only depleted by evapotranspiration, can be calculated from storage change over the entire soil profile.

When percolation occurs in the subsoil, the depth of the horizontal "watershed" has to be determined (above that: soil moisture depletion via evapotranspiration, below it via percolation) with tensiometer measurements (Dyck and Peschke, 1995). (Zero-plane displacement, Fig. 6).

When lateral fluxes cannot be excluded and longer time periods are considered ET can be calculated as (Rana and Katerji, 2000):

$$P + Ir + W - Ro - Dr \pm \Delta S \tag{3}$$

with Ir: irrigation, W: upward water transfer from the water table, Ro: runoff, Dr: drainage, ΔS: storage change. Can be applied to small plots to catchments of ≈ 10 km^2, periods ranging from 1 week to years. Simplifications and uncertainties in the measurements, esp. of the terms Ro and Dr make it unsuitable for precise ET measurement. Accuracy of soil moisture measurements depends on spatial and temporal resolution of soil moisture measurements, representativity of samples (Rana and Katerji, 2000).

Soil moisture measurements in arid climates are especially prone to measurement errors: cracks in soil can prevent contact between soil and probes, high clay content difficult for measurements with TDR/FDR probes or neutron scattering (Rana and Katerji 2000 and studies cited herein).

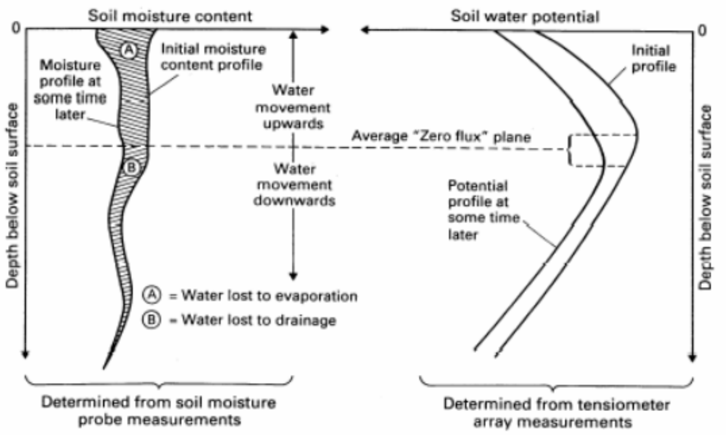

Figure 6: Estimation evapo(transpi)ration from soil moisture depletion / Zero plane displacement method, from Shuttleworth (2007).

1.4.4 Meterological measurements

Calculation of evaporation from meteorologic measurements:

Water vapor budget method (Hipps and Zehr, 1995; Sill et al., 1984): Calculation of ET of a controll volume from measurement of the water vapor profile up- and downwind of the parcel:

$$ET = \frac{\lambda}{F} \int_0^z u\rho(z) \left[q_d(z) - q_u(z)\right] dz \tag{4}$$

with λ: latent heat of vaporization, F: length of the fetch, u: mean wind speed over the profile, $\rho(z)$: air density at height z, $q_d(z)$ and $q_u(z)$: down- and upwind specific humidity at height z.

Prueger et al. (1996) obtained results with this method that were generally 10 % lower than ET measured with Eddy correlation systems.

Method seems not to be used a lot, the papers that are gicen as references are cited just 7 and 12 resp. times (Google scholar).

1.4.5 Eddy-correlation measurements

Measurements of surface energy fluxes: evaporation, sensible heat, momentum fluxes, CO_2 fluxes; on towers or aircrafts ((**Desjardins et al., 1997; Samuelson and Tjernstrom, 1999; Stephens et al., 2000; Mahrt et al., 2001; Song and Wesely, 2003; Prueger et al., 2005**, all cited in Anderson et al. (2007a)).

Towers: temporal continuous but, spatially discrete measurement, airplanes: other way round (Anderson et al., 2007a).

The vertical flux of water vapor is calculated as the product of variations of specific humidity q and vertical windspeed u_z around their mean values (Dyck and Peschke, 1995):

$$ET = \rho \cdot \overline{q}' \cdot \overline{u}'_z \quad [kg\, m^{-2} s^{-2}] \tag{5}$$

with ρ: density of the air $[kg\, m^3]$, $\cdot\overline{u}'_z$: temporal mean of the differences between the vertical component of windspeed and it's mean, $\overline{q}'$: temporal mean of the differences between specific humidity and it's mean.

Necessary mesurements: u_z and q at high frequency (10 - 20 Hz)with sonic anemometers and fast response hygrometers (Dyck and Peschke, 1995; Rana and Katerji, 2000).

Sources of errors (see also Fig 7):

- Systematic underestimation (Shuttleworth, 2007; Anderson et al., 2007a)
- deviations from theoretical assumptions (Foken and Wichura, 1996):
  - temporal (statistic) stationarity of the measured processes (X: wind speed, temperature etc): $\partial X/\partial t = 0$
  - stationarity along the horizontal axis (homogeneity): $\partial X/\partial x = 0$
  - validity of the mass conservation equation: $\partial w/\partial t = 0$ and $\overline{w} = 0$ with w: vertical wind speed
  - negligible density flux
  - momentum flux and temperature flux do not change with height more than 10 - 20 % of total flux
  - Furthermore: fulfillment of the Reynolds postulate and statistical assumptions
- statistical signal processing errors (time avaraging, aliasing)
- distortion of the flow caused by the sensors itself (Fig. 7)
- meteorological problems (Fig. 7)
- heterogeneity of fluxes in time (below time step heterogeineity) and space (heterogeneity within the footprint) (Bohn and Vivoni, 2015)
- complex topography (Bohn and Vivoni, 2015).

The method is often used as a reference for other measurement methods, model performance. For this procedure, uncertainties inert in the method shoud be considered.

Regional / global measurement networks, e.g. Ameriflux, EuroSiberiaFlux, Asiaflux, Fluxnet (Baldocchi et al., 2001).

Literature: Aubinet et al. (2012)

Good performance in semi-arid regions, density correction is especially important under these conditions (Rana and Katerji, 2000).

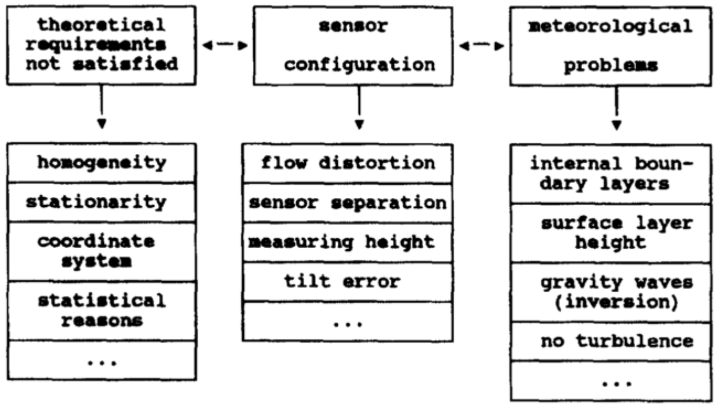

Figure 7: Possible sources of error in eddy correlation measurement of evapotraspiration. From Foken and Wichura (1996).

1.4.6 Scintillometer measurements

Scintillation method can provide area avaraged surface fluxes of sensible heat (H) and water vapor fluxes (ET) at large scales (Distances up to 10 km). Radio wavelength scintillometers (RWS) are most sensible to water vapor fluxes. Scintillometers operating in visible light wavelength measure sensible heat fluxes.

Functionality: "The transmitter part of the scintillometer emits a beam of electromagnetic radiation with a certain wavelength along the surface at height z_s and path length L to the receiver part of the system. At the receiver side the intensity fluctuations of the electromagnetic signal (called scintillations) are measured ($\sigma^2_{ln\,I}$), which are caused by atmospheric turbulence in the path of propagation." (Meijninger et al. (2002), fig. 8). $\sigma^2_{ln\,I}$ is used to calculate the structure parameters of temperature (C_T^2) and humidity (C_Q^2) which is used to calculate fluxes of heat and water vapor with Monin-Obukhov Similarity Theory (MOST). Therefore, measurements at two wavelengths are necessary.

In theory the landscape in the footprint has to be homogenous, in practice it was shown to work for heterogenous landscapes as well. For heterogenous areas, the path of the scintillometer has to be higher than the blending height which depends on the length of landscape's patches in wind direction. (Meijninger et al., 2002).

Other references: Andreas (1989); Ward et al. (2015a,b); Guyot et al. (2009, 2012) (The latter two in Sudano-Sahelian climate with strong seasonality of rainfall, pronounced dry season, African monsoon)

1.4.7 Bowen Ratio

Bowen (1926)

Bowen Ratio Bo is the ratio of heat flux H to evaporative flux ET:

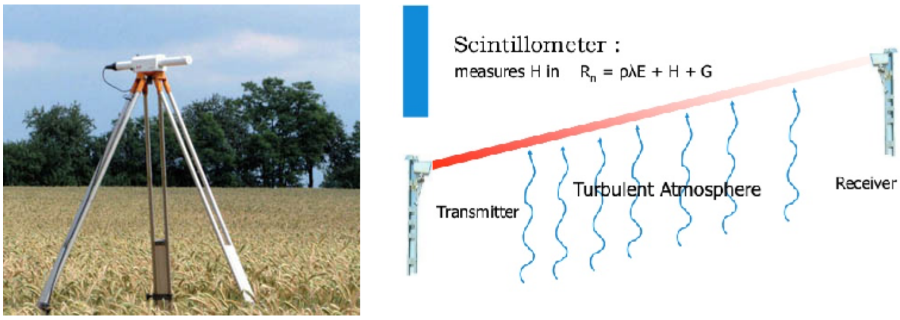

Figure 8: Scintillometer measurement of surface fluxes.

$$Bo = \frac{H}{\lambda ET} \tag{6}$$

with λ: latent heat of vaporization and ET the mass $[g]$ of water evaporated (Lewis, 1995). Thus, evaporation ET can be calculated as:

$$ET = \frac{R_n - G}{\lambda(1 + Bo)} \tag{7}$$

with R_n: net radiation, can be measured with a net radiometer and G: ground heat flux, measureable with soil heat flux plates.

The Bowen ratio can be determined with a Bowen ratio observing system: Measurement of temperature and vapor pressure at two heights, calculation as:

$$Bo = \frac{\Delta T}{\Delta e} \tag{8}$$

with ΔT: temperature difference and Δe: difference in vapor pressure.

Method successfully applied in semi-arid regions (Rana and Katerji 2000 and studies cited herein). In these regions, especially the measurement of Δe has to be very accurate (as is usually very small compared to ΔT), this can pose technical problems (high requirements on hygrometer accuracy) esp. in the dry season air humidity is very low (Rana and Katerji, 2000).

1.4.8 Isotopic compounds

e.g. Yepez et al. (2003); Moreira et al. (1997), review papers: Griffis (2013); Soderberg et al. (2012); Horita et al. (2008); Dawson et al. (2002)

Water evaporated from soil surfaces is depleted in heavy isotopes, different isotopic composition than soil water. Transpiration on the other hand doesn't change isotopic composition once an isotopic steady state (ISS) is reached, thus the two fractions have significantly different compositions. Before ISS is reached, there is a fractioning in the leaf, thus on the short term water vapor composition can deviate from the steady state, thus, analysis of different sources of transpiration possible (Yepez et al., 2003).

Advantage: Evapotranspiration can be separated into evaporation and transpiration (Kool et al., 2014) or even into different transpiration portions from different parts of the canopy. Good correlation with Eddy Correlation measurements (Yepez et al., 2003). Applicable at large scales, esp. suitable in dry areas where evaporation is significant (> 10 %, Kool et al. 2014)

2 Remote sensing

Advantages: Spatial integration over heterogenous surfaces, routine-generation of data series (Kalma et al., 2008).

Data that can be obtained via remote sensing:

- Eddy correlation data from airplanes.
- Thermal infrared radiation (TIR) e.g. satellite sensors such as Landsat, MODIS, AVHRR, ASTER; derivation of surface temperature
- Components of the radiation budget; derivation of net radiation R_n
- Vegetation indices such as normalized difference vegetation index (NDVI) and enhanced vegetation index (EVI); derivation of leaf are index (LAI)

Review of studies that estimate evapotranspiration with remotely sensed data in Kalma et al. (2008), see sec. 3.8.1. Main findings: Mean RMSE of 30 published validation studies is about 50 Wm^{-2}, relative errors of 15 - 30 %. More complex physical approaches not neccessarily more accurate than empirical approaches.

References e.g. Githui et al. (2012); Jhorar et al. (2011); Anderson et al. (2007b); Allam et al. (2016); Tang et al. (2010)

3 Calculation approaches

Overview: `http://www.climate-service-center.de/033633/index_0033633.html.de` (in German).

Several methods implemented in R package Evapotranspiration (Guo et al., 2016).

Comparison of different methods e.g. in Oudin et al. (2005); Seiller and Anctil (2016). Evaluation with the performance of rainfall-runoff models applied with differently calculated ET.

Some conclusions: Different formulas produce very different timeseries of ET, esp. in the summer months (Seiller and Anctil, 2016). Model performance is however strikingly similar for most of the formulas applied, low sensitivity of the models to the chosen ET representation (Oudin et al., 2005). Simpler termperature- or radiation-based methods yield similar or even better results than the more complicated combinational formulas of the Penman-type (Fig.

9). Possible reasons: higher resolution of available measurements, adaptation of the models via calibration, elimination of systematic biases (Oudin et al., 2005; Seiller and Anctil, 2016).

Andréassian et al. (2004) found surprisingly low differences between model efficiency when different levels of accuracy of evapotranspiration data are used as input to two hydrological models are used. This shows the adaptative capacity of rainfall-runoff models to adapt to biased ET data.

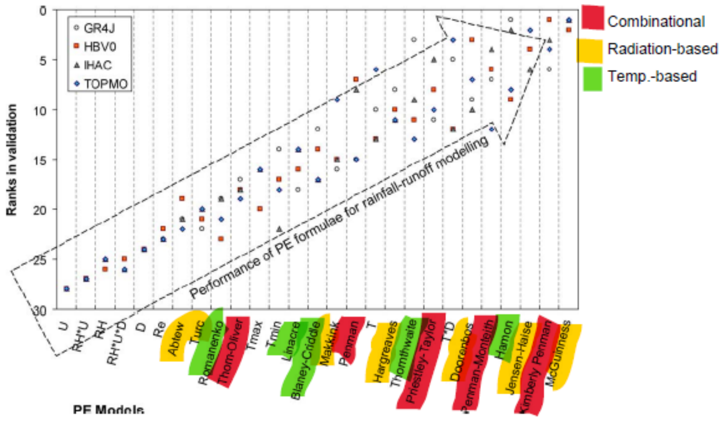

Figure 9: Performance of four rainfall-runoff models run with evaporation derived from 27 formulas. From Oudin et al. (2005).

Different approaches according to Xu and Singh (2001): water budget, mass transfer, combinational, radiation-based and temperature-based:

3.1 Water budget methods

ET calculated as:

$$ET = P - Q \tag{9}$$

with Q: discharge. Only applicable for longer timesteps ($\approx$ 1 a) where storage changes ΔS can be neglected, not differentiated into different components. Major sources of error: deriving catchment precipitation, watershed boundaries (esp. when Groundwater is important), reliable discharge measurements. Method is commonly used to derive long-term mean evapotranspiration for river basins (Conradt et al., 2013). In the study by Conradt et al. (2013) the method doesn't correlate well with other two methods (Modelled in SWIM with Turc-Ivanov approach, calculated with SEBAL algorithm).

Application e.g. in Conradt et al. (2013); Allam et al. (2016).

3.2 Mass-transfer methods

One of the oldest methods. Advantages: simplicity and reasonable accuracy (Singh and Xu, 1997). Evapo(transpi)ration is calculated as a function of wind speed u, temperature T and water vapor deficit $(e_s - e)$ or relative humidity q_r. Based on Daltons equation (Dalton, 1802) for free water surfaces:

$$ET = \frac{1}{r_a}(e_s - e) \tag{10}$$

with r_a: aerodynamic resistance, $(e_s - e)$: water vapor deficit.

E.g. equations proposed by Penman (1948); Romanenko (1961), these and other equations given in Singh and Xu (1997).

This approach is used in the analytical model Cupid-DPEVAP (Thompson et al., 1993) for the calculation of evaporation:

$$E = h_v(\frac{M_v}{RT_{abs}})(e_0 - e_z) \tag{11}$$

with h_v: surface vapor transfer coefficient, M_v: molecular weight of water, R: ideal gas constant, T_{abs}: absolute temperature $[K]$, e_0 and e_z: vapor pressure at the surface and at height z.

Also used in the numerical model SWEAT (Daamen and Simmonds, 1994) for separate modelling of evaporation, transpiration and evapotranspiration (description in Kool et al. 2014).

3.3 Energy balance methods

Residual approach: latent heat flux (λET) is calculated as the residual of the energy balance equation:

$$\lambda ET = R_n - G - H \tag{12}$$

with R_n: net radiation, G: ground heat flux, H: sensible heat flux. R_n is usually derived from remotely sensed or measured data of the components of the radiation budget $R_n = R_{s,in} - R_{s,out} + R_{l,in} - R_{l,out}$, with the subscript s and l denoting short- and long-wave radiation and *in* and *out* incoming and outcoming radiation (Kalma et al., 2008). G depends on the soil's thermal conductivity and temperature gradient, cannot be measured remotely only with soil heat flux plates, is either assumed to be a constant ratio of R_n (5 - 20 %) or estimated as a function of parameters such as solar zenith angle, vegetation cover, LAI, NDVI, soil moisture (Kalma et al., 2008). Rough estimate of the combined effect of error in R_n and G: ± 10-20 % (Kalma et al., 2008).

H has to be calculated e.g. using equation 13 (Kalma et al., 2008):

$$H = \rho C_p \frac{T_{aero} - T_a}{r_{ah}} \tag{13}$$

with ρ: air density, C_p: specific heat of air, T_{aero}: aerodynamic surface temperature, T_a: air temperature, r_{ah}: aerodynamic resistance to sensible heat transfer. r_{ah} is sometimes assumed to be r_a (see sec. 5.2.1) or can be calculated as a function of local wind speed, surface roughness length, atmospheric stability conditions:

$$r_{ah} = \frac{1}{k^2 u(z)}(\ln\frac{z-d}{z_{0h}} - \Psi_h \frac{z-d}{L})(\ln\frac{z-d}{z_{0m}} - \Psi_m \frac{z-d}{L}) \qquad (14)$$

where k: von Karman's constant, $u(z)$: windspeed at reference height z, d: displacement height, z_{0h} and z_{0m}: roughness lengths for sensible heat and momentum flux, functions of canopy height h_c, Ψ_h and Ψ_m: stability correction functions for sensible heat and momentum flux, L: Monin-Obukhov length.

Constraits of this approach include the uncertainty ot T_{aero}, fluctuations in r_{ah}, thus calibration (e.g. Bastiaanssen et al. (1998)) or adaptation of frmulas 13 and 14 (several versions given in Kalma et al. (2008)) are necessary. Furthermore, lateral fluxes (advection) are usually neglected but can contribute up to 90(!) % of the energy available for evapotranspiration in highly heterogenous irrigated arid landscapes (Prueger et al., 1996).

Energy and water balance are implemented e.g. in the numerical model ENWATBAL (Lascano et al., 1987) that computes water and energy balances at the soil and the canopy, seperate treatment of evaporation and transpiration (Kool et al., 2014).

Two source energy balance model TSEB also computes ET, E and Tr with two separate equations for the canopy and the soil from surface temperature data that can be obtained via remote sensing (Kool et al., 2014).

3.4 Combinational methods:

3.4.1 Penmen

Semi-empirical approach to calculate potential evapotranspiration, derived from the energy balance and aerodynamic methods, relies on standard measurements, developed for humid, vegetated surfaces, original paper for open water, bare soil and grass (Penman, 1948). Does not consider plant physiology, which is included by Monteith (Penman-Monteith eq.). "Considered as the most physically satisfying by many hydrologists (Jensen et al., 1990; Shuttleworth, 1993; Beven, 2001)." (Oudin et al., 2005)

$$ET = \frac{\Delta A' + \gamma[6.43(1 + 0.536\, u)D]/\lambda}{\Delta + \gamma} \quad [mm\, d^{-1}] \qquad (15)$$

with Δ: rate of change saturated vapor pressure, A': energy available for evaporation from the free water surface $[mm\, d^{-1}]$, γ: psychromatic constant, u: wind speed, D: vapor pressure deficit at 2 m $[kPa]$, λ: latent heat of vaporization of water (stated in Shuttleworth (2007))

3.4.2 Priestley-Taylor

Derived from the Penman equation by Priestley and Taylor (1972), advection term replaced by a fraction of the radiative term, less measurements neccessary, also aplicable for conditions when soil moisture limits evapotranspiration (Shuttleworth and Wallace, 1985). Xu and Singh (2000): only for wet surfaces.

$$\lambda ET = 1.26 \frac{\Delta A'}{\Delta + \gamma} \tag{16}$$

Disadvantage: too simple (Shuttleworth, 2007).

3.4.3 Penmen-Monteith

Widely used, physically based combination equation. Introduction of plant parameter stomatal conductance into Penman's equation based on the energy balance. First approach that combines energy balance and plant physiology. ET is restricted by aerodynamic resistence and canopy resistance.

$$\lambda ET = \frac{\Delta A' + (\rho \cdot c_p \cdot D)/r_s}{\Delta + \gamma(1 + r_s/r_a)} \quad [Wm^{-2}] \tag{17}$$

abbreviations as in Penman eq., ρ: densitiy of the air, c_p: specific heat of air at constant pressure, r_s: stomatal resistance, r_a: aerodynamic resistance.

Sensitivity analyses of the formula conducted by Beven (1979), Rana and Katerji (1998) (in semi-arid southern Italy), McCuen (1974), Saxton (1975); main findings: High sensitivity to resistances (Beven, 1979); In (semi-) arid climates sensitivity depends on plant height and water status (Rana and Katerji, 1998): For short, well watered grass the formula is mainly sensitive to climatic variables: available energy and -under certain conditions - vapor pressure deficit and aerodynamic resistance. For tall, water stressed plants almost all error in ET can be attributed to erroneous representation of canopy resistance, a further sensitive parameter is vapor pressure deficit.

Main disadvantages:

- High data demand,
- High dependence of model performance on the accuracy of the estimation of the resistancies, esp. canopy resistance (Beven, 1979). Several empirical or semi-empirical formulas are used to calculate r_s and r_a (see sec. 5)
- Simplifications: linearization of the saturation vapour pressure curve, neglecting the dependency of net irradiation on surface temperature (Schymanski and Or, 2016)
- The equation is developed for the leaf scale and for data at short time steps, upscaling to the canopy scale and use of daily or monthly data require various empirical corrections (Schymanski and Or, 2016).
- Original equation only valid for amphistomatous leaves (stomata on both sides of the leaf), adaptation for hypostomatous leaves (stomata only on the lower side of the leaf) by Monteith and Unsworth (2013), corrected by Schymanski and Or (2016).

Several studies reviewed in Oudin et al. (2005) indicate that the method is not necessarily the best choice for hydrological modelling: Simpler formulas produce similar or even better medelling behaviour, higher resolution of available measurements when simpler temperature- or radiation based methods are applied.

Criticized e.g. by Morton (1994) (cited in Oudin et al. (2005)): "It seems likely that the use of the Penman - Monteith equation to estimate evaporation from hydrologically significant areas has no real future, being merely an attempt to force reality to conform to preconceived concepts derived from small wet areas."
Experiments conducted by Schymanski and Or (2016) in controlled environment (all parts of the energy balance measured, artificial leaves with known stomatal conductance) are not accurately reproduced by the Penman-Monteith equation, better reproduction with a numerical model as well as an analytical equation (eq. 20) proposed by the same authors and the numerical model by Ball et al. (1988).

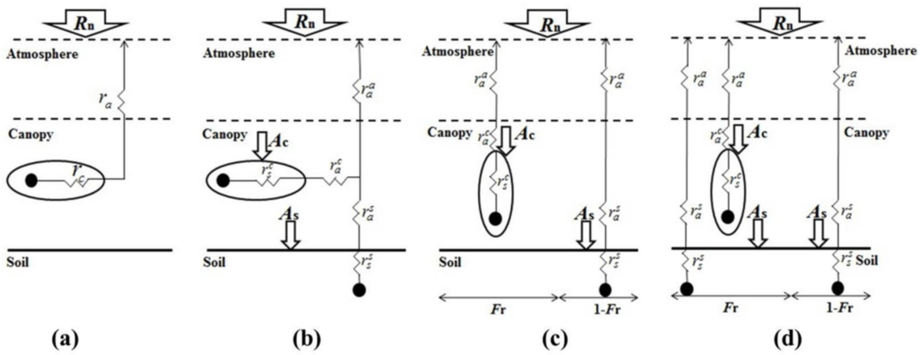

Figure 10: Different concepts of sources and resistances, from Lu et al. (2014).

Different concepts of sources and resistances:

Big leaf approach: Original equation assumes a single source area (Big-Leaf approach, fig. 10a). Assumption of a closed canopy, not suitable for patchy vegetation, no differentiation between evaporation, transpiration and interception. Further assumption: Sources of heat and water vapor are located at the same level in the canopy, not the case in tall and / or sparse canopies (Finnigan et al. (2003), Foken and Wichura (1996), cited in Ershadi et al. (2015)) .

Multi-layer and multi-source approaches: Two-, three- or multi-source models (as opposed to the big leaf approach), e.g. Shuttleworth and Wallace (1985); Choudhury and Monteith (1988); Shuttleworth and Gurney (1990); Mu et al. (2011); Lu et al. (2014) include evaporation from soil at sites with sparse vegetation. Differences between the multiple layer approach (fig. 10b, coupled, resistances in series), the multiple patch approach (fig. 10c, uncoupled, parallel resistances) and hybrid dual source approaches (fig. 10c) (Lu et al., 2014).

Shuttleworth-Wallace-Model: Shuttleworth-Wallace-Model sparse-crop model (SW, Shuttleworth and Wallace, 1985, fig. 10b) assumes uniform distribution of vegetation. Total evapotranspiration is a weighted mean of ET from the plants and the soil:

$$ET = C_{pl} ET_P + C_s ET_S \tag{18}$$

with C_{pl} and C_s: Parameters describing the plant's or soil's aerodynamic resistence. Evaporation from bare soil and evaporation from a closed canopy are asymptotic limits of eq. 18. Good description of the model and formulas for ET_S and ET_P e.g. in Ershadi et al. (2015).

Advantages: allows for ET partitioning, regards different sources of fluxes, allows weigthing them, considered accurate (Kool et al., 2014). Found to reproduce ET measurement on a semi-arid sudy site significantly better that the big-leaf approach by Stannard (1993).

Disadvantages:

- Assumption of a horizontally homogeneous atmosphere, thus no advective effects, mesoscale circulation patterns.
- Neglectance of interception
- Hard to parameterize

Strong deviations between observed and simulated values found in arid regions by Gao et al. (2016), and Zhu et al. 2007 (cited in Gao et al. 2016), possible explanation: substantial advective efects in the atmosphere.

Brenner and Incoll 1997 Three-source model, considers transpiration from the plant ET_p, evaporation from the soil under the plant ET_s and evaporation from bare soil ET_{bs}:

$$ET = f_c(C_{pl} ET_P + C_s ET_s) + (1 - f_c)(C_{bs} ET_{bs}) \tag{19}$$

with f_c being the fractinal vegetative cover.

Resistances can be considered as parallell resistances or resistances in series.

Mu et al., 2011: Total evapotranspiration is differentiated into evaporation, transpiration and interception, all are seperately calculated with Penman-Monteith equations whith resistances that are specified for each source. The three sources are weighted based on fractional vegetation cover f_c and relative surface wetness f_w. Original reference: Mu et al. (2011), good description: Ershadi et al. (2015).

Advantages: Parameterization of resistances doesn't require wind speed and soil moisture (Ershadi et al., 2015).

Other variations of the Penman-Monteith equation: 4 different equations to calculate only evaporation from soil as a function of r_s^s (soil surface resistance, see section 5.1.5), scaling parameters α (ratio of actual water vapor pressure to saturated water vapor pressure) and β (ratio of actual evaporation to potential evaporation), or ET_{max} (threshold evaporation) given in Merlin et al. (2016).

3.4.4 Schymanski and Or (2016)

Equation proposed by Schymanski and Or (2016), based on a generalization of Penman's approach and consideration of the dependence of the longwave component of the energy balance equation on leaf temperature (unlike Penman's and Penman-Monteith equations):

$$ET = \frac{c_H(\Delta_{T_a}(T_l - T_a) + P_{was} - P_{wa})}{\gamma} \tag{20}$$

With c_H: sensible heat transfer coefficient, Δ_{T_a}: slope of the saturation vapor pressure curve at air temperature T_a, T_l: leaf temperature, P_{was}: Saturation vapour pressure at air temperature, P_{wa}: Vapour pressure in the atmosphere. Leaf temperature T_l is either measured (e.g. with infrared sensors) or calculated as:

$$\begin{split} T_l = (R_s + c_H T_a + c_E(\Delta_{T_a} T_a + P_{wa} - P_{was}) + \\ a_{sh}\epsilon_l\sigma(3T_a^4 + 4T_w^4))\frac{1}{c_H + \Delta_{T_a} + 4a_{sh}\epsilon_l\sigma T_a^3} \end{split} \tag{21}$$

with a_{sh}: fraction if projected area exchanging sensible heat with the air, ϵ_l: long wave emmissivity of the leaf surface, T_w: radiative temperature of objects surrounding the leaf.

3.5 Radiation-based methods

Most radiation based methods take the folloing form (Xu and Singh, 2000):

$$\lambda ET = C_r(wR_s) \quad or \quad \lambda ET = C_r(wR_n) \tag{22}$$

with C_r: coefficient, $f(u, q_r)$, w: weighting factor, $f(Temp., altitude)$.

Xu and Singh (2000) compared five radiation-based formulas with measured evaporation pan data in Switzerland, Abtews equation performed best when coefficients proposed by the original references were used. After calibration of the coefficients, Makkink and Priestley-Taylor formulas performed best. Abtew formula is recommended when no further data (other than radiation) is available.

3.5.1 Turc's formula

Empirical equation for the calculation of potential evapotranspiration in 10 d periods, developed for France and northern Africa (Turc, 1961), Correction factors can be used for other regions. Formula: see below.

3.5.2 Turc-Ivanov

For colder regions; use of Turc's formula for days with avarage temperature $T > 5°C$, Ivanovs formula (some source in Russian, cited e.g. in Conradt et al., 2013) for days with a lower avarage temperature:

$$ET_{pot} = \begin{cases} 0.0031 \cdot \Omega \cdot (R_n + 209.4) \cdot (\frac{T}{T+15}) for \quad T \geq 5°C \\ 0.000036 \cdot (T+25)^2 \cdot (100 - q_r) for \quad T < 5°C \end{cases} \tag{23}$$

with T daily average temperature, R_n net radiation, rh relative humidity, Ω dimensionless factor, varies for each month. Implemented e.g. in the SWIM model (Conradt et al., 2013).

3.5.3 Makkink

Based on measurements on grassland in the Netherlands, can be used for sub-daily time steps.

$$ET_{pot} = 0.61 \frac{\Delta}{\Delta + \gamma} \frac{R_n}{58.5} - 0.12 \tag{24}$$

Disadvantage: influence of the wind is not considered.

3.5.4 Jensen-Haise

Combination of measured evapotranspiration data from irrigated areas in the western USA with radiation data. Derivation of a formula based on 1000 samples for irrigated areas in arid or semi-arid regions (Jensen and Haise, 1965):

$$\lambda ET = C_t(T - T_x)R_s \tag{25}$$

with C_t: temperature constant (=0.025), T_x: -3°C.

3.5.5 Hargreaves

Several equations, derived from lysimeter measurements of cool season Alta fescue grass in Davies, California, e.g. (cited in Xu and Singh (2000)):

$$\lambda ET = 0.0135(T + 17.8)R_s \tag{26}$$

Can be applied with remote sensing data (El-shirbeny et al., 2016).

3.5.6 Doorenbos and Pruitt

Adaptation of Makkink method, recommended over Penman method when data for wind and humidity are not available (Xu and Singh, 2000):

$$ET = a(\frac{\Delta}{\Delta + \gamma} R_s) + b \tag{27}$$

with a: adjustment factor, $f(u, rh)$ and b = -0.3 $mm\, d^{-1}$. (So u and rh do have to be known??)

3.5.7 McGuinnes and Bordne

Calculation of monthly potential ET, based on lysimeter measurements in Florida:

$$ET = [(0.0082T_F - 0.19)(R_s/1500)]2.54 \tag{28}$$

with T_F: temperature in Fahrenheit.

3.5.8 Abtew

$$ET = K_A \frac{R_s}{\lambda} \tag{29}$$

with K_A: dimensionless coefficient

3.5.9 Priestley-Taylor

See sec. 3.4.2.

3.6 Temperature-based methods

Xu and Singh (2001): Most temperature-based equations take the form

$$ET = cT^a \tag{30}$$

or

$$ET = c_1 DL\, T(c_2 - c_3 h) \tag{31}$$

where h is a humidity term, c, a, c_1, c_2 and c_3 are constants and DL is day length.

3.6.1 Thornthwaite

Original reference: Thornthwaite (1948). Developed from the correlation between mean monthly temperature and evapotranspiration determined from the water balance of valleys with sufficient available water for potential evaporation.

$$ET = 16(\frac{d_l N}{360})(\frac{10T_m}{I_h})^{K_T} \tag{32}$$

with heat index I_h summed up over a 12 month period: $I_h = \sum_{n=1}^{12}(\frac{T_m}{5})^{1.514}$, T_m: mean monthly temperature and $K_T = 0.49239 + 1.792I10^2 - 0.771I^2 10^{-4}$, d_l: duration of avarage monthly daylight, N: number of days in a given month.

Widely used because it needs only tmperature as input. Widely misused for irrigated arid and semi-arid areas (Xu and Singh, 2001).

3.6.2 Linacre

Simplification of Penman's equation, for well-watered areas with an albedo of aprox. 0.25:

$$ET = \frac{500T_h/(100 - Lt) + 15(T_a - T_d)}{80 - T_a} \tag{33}$$

where $T_h = T_a + 0.006h$,T_a: air temperature, h: elevation, Lt: latitude, T_d: dew point.

3.6.3 Blaney and Criddle

Reference: Blaney and Criddle (1950). Developed in the southwestern USA, based on lysimeter measurements, widely used.

$$ET = f_{BC}\, p(0.46T + 8.13) \tag{34}$$

with f_{BC}: a monthly coefficient, based on vegetation, location and season, varies from 0.5 (orange tree) to 1.2 (dense natural vegetation); p: percentage of daytime hours to total time of the calculation timestep (day or month).

3.6.4 Kharrufa

Developed for arid regions. Reference: Kharrufa (1985).

$$ET = 0.34p\,T^{1.3} \tag{35}$$

3.6.5 Haude

Widely used in Germany, based on numerous measurments in northern Germany, simple, daily values with high uncertainty, should be summed up to monthly values (Dyck and Peschke, 1995).

$$ET_{pot} = f_H(e_s - e)_{14:00} \tag{36}$$

with f_H: proportionality factor, given in a table for each month, $(e_s - e)_{14:00}$: saturation deficit at 2 pm, calculated as a function of temperature and relative humidity with the Magnus formula: $e_s = 611.2 \exp \frac{17.62T}{243.12+T}$ and $e = q_r e_s$.

3.6.6 Oudin

Based on model efficiency of 4 rainfall-runoff models of 308 catchments in different climates with potential evapotranspiration calculated with 27 formulas, proposal of a formula adapted to rainfall-runoff-models, simple (requires only mean air temperature from long term avarages), efficient (Oudin et al., 2005):

$$ET_{pot} = \begin{cases} \frac{R_e}{\lambda\rho}\frac{T_a+5}{100} & for \quad T_a + 5 > 0°C \\ 0 & otherwise \end{cases} \tag{37}$$

with R_e: extraterrestrial radiation, function of latitude and Julian day.

3.6.7 Others

Other temperature based equations given in Xu and Singh (2001): Hargreaves (Hargreaves, 1975; Hargreaves and Samani, 1982, 1985), Hamon (Hamon, 1960), Romanenko (Romanenko, 1961).

3.7 Reference evapotranspiration

Parallel, two-step approach: 1) Determination of reference evapotranspiration ET_0 for a reference crop (short grass, alfalfa) without water limitation with (simplified) Penman-Monteith equation, calculation of crop potential evapotranspiration by multiplication with a crop coefficent K_c Allen et al. (1998). 2) Calculation of actual evapotranspiration by multiplication with relative evapotranspiration based on soil moisture (Doorenbos and Pruitt, 1977; Allen et al., 1998).

Advantages:

- Widely used, especially in agricultural and irrigation hydrology
- much data on crop coefficients available

Disadvantages:

- Not easily applicable to heterogenous surfaces
- Crop coefficients for natural environments unknown
- High uncertainty of the relation between soil moisture and relative evapotranspiration (Gasca-Tucker et al. (2007) and other sources cited by these authors)
- discrepancy between literature values for K_c and locally derived values that depend on seasonality (growth stages), site and climate (Rana and Katerji, 2000)

Based on a review of case studies that use the method in non-irrigated semiarid areas, Mata-González et al. (2005) conclude that ET is typically overestimated when plants encounter suboptimal conditions of soil water, because it doesn't consider stomatal regulation and plant adaptation to draught. Thus the method is not recomended in these environments.

Penman-Monteith equation is simplified to the reduced form known as FAO56-PM equation (Allen et al., 2006):

$$ET_0 = \frac{0.408\Delta(R_n - G) + \gamma \frac{C_n}{T_m + 273} u_2 (e_s - e)}{\Delta + \gamma(1 + C_d u_2)} \tag{38}$$

with T_m: mean daily or hourly temperature, C_n and C_d: coefficients that vary with the calculation time step, reference crop (grass or alfalfa) and time of day, values given in Allen et al. (2006), u_2: wind speed at 2 m height.

Attempt to convert crop coefficients to surface resistances by Shuttleworth (2006).

The dual-K_c approach divides K_c into a plant component K_{cb} and a soil component K_e, this approach is the most common method for ET partitioning (Kool et al., 2014).

3.8 Others

3.8.1 Methods developed for remotely sensed data

Methods using the difference between surface and air temperature: Estimation of daily evapotranspiration as:

$$\lambda ET_d = R_{n,d} - B(T_s - T_a)^n \tag{39}$$

with $R_{n,d}$: daily net radiation, T_s: remotely sensed surface temperature, T_a: air temperature in 50 m height, both temperatures at the time of satellite overpass. B and n: parameters, closely related to fractional cover f_c. B ranges from 0.015 (bare soil) to 0.065 (fully vegetated surface), n from 1.0 (bare soil) to 0.65 (full cover, Carlson et al. (1995), cited in Kalma et al. (2008)). Requires local calibration (Kalma et al., 2008).

Methods using the temporal rate of change in surface temperature in atmospheric boundary layer models: e.g. Wetzel et al. (1984); Anderson (1997); Anderson et al. (2007b,a); Norman et al. (2000)Advantage over the difference between the difference between surface and air temperature: Offset between the measurments of T_s and T_a are cancelled out, reduced need for absolute accuracy of temperature measurements (Kalma et al., 2008).

SEBAL: Surface Energy Balance Algorithm for Land (Bastiaanssen et al. (1998), described e.g. in Kalma et al. (2008); Conradt et al. (2013)), derived from surface energy balance (eq. 12). Developped for the local scale, relatively flat landscapes. Uses remotely sensed surface temperature, surface reflectivity and NDVI. Calibration using the wettest ($ET >> H$) and the dryest pixel ($H >> ET$)

Advantage: requires few ground level observations.
Other references: Zheng et al. (2016)

METRIC Mapping EvapoTranspiration with high Resolition and Internalized Calibration (Tittebrand et al., 2005; Allen et al., 2007a,b). Derived from SEBAL for irrigated crops.

Others: Other methods described in Kalma et al. (2008):

S-SEBI: Simplified Suface Energy Balance Index (Roerink et al., 2000): Derivation of the evaporative fraction $\Lambda_i = \lambda ET/(R_n - G)$ from remotely sensed surface and reflectivity data.

Link of evaporative cooling and the negative correlation between remotely sensed surface temperature and NDVI used by Hope et al. (1986); Nemani and Running (1989).

Several studies that correlate evapotranspiration with vegetation indices are reviewed in Glenn et al. (2007), R^2 values of about 0.81, this relationship is proposed for upscaling ET measurements to larger scales (Kalma et al., 2008).

3.8.2 Rutter

Interception model (Rutter et al., 1971)

3.8.3 Numerical models

e.g. in Ball et al. (1988), Schymanski and Or (2016).

4 Water limitation

Implemented with scaling parameters (e.g. Wetzel and Chang (1987)), relation between actual and potential evapotranspiration, complementary relationship (Bouchet, 1963)), resistances (Jarvis, 1976).

Relation between actual (AET) and potential evapotranspiration (PET) can be calculated as a function of plant and soil characteristics and available soil water, e.g. with the following equation proposed by Baier and Robertson (1966):

$$AET_i = \sum_{j=1}^{n} K_{r,j,i} \frac{S_{j,i-1}}{C_{w,j}} C_{s,j} PET_i e^{-wPET_i - \overline{PET}} \quad (40)$$

with K_r: crop specific root coefficient, S: available soil water, can be obtained e.g. from soil water simulation models (De Jong and Bootsma, 1996; Leenhardt et al., 1995), C_w: water holding capacity, C_s: soil coefficient, w: empirical adjustment factor, $\overline{PET}$: long-time avarage PET. Subscripts i and j refer to time and depth zone respectively.

The ratio ET_{act}/ET_{pot} can be determined from crop water stress index (CWSI), which in turn can be derived from remotely sensed canopy temperature and air temperature (Kalma et al., 2008).

5 Resistances

Very important for model parameterization, high sensitivity of evapotranspiration models to resistances, considerable source of uncertainty (Beven, 1979; McCabe et al., 2005; Ershadi et al., 2015). Direct measurement are difficult to impossible, different calculation approaches.

5.1 Surface resistances

Crucial parameter in the Penman-Monteith model, difficult to measure or estimate, very dependent on soil, climate and crop characteristics (Rana et al., 1997). Values for surface resistance are often obtained via inverse modelling with the Penman-Monteith equation and measured evapotranspiration (e.g. Rana and Katerji (1998); Brisson et al. (1998)) following Baldocchi et al. (1991) and Tolk et al. (1996).

5.1.1 Single surface resistance

Jarvis surface resistance parameterization method: described e.g. in Ershadi et al. (2015):

$$r_s = \frac{r_s^{min}}{LAI \cdot F_1 \cdot F_2 \cdot F_3 \cdot F_4} \tag{41}$$

with r_s^{min}: minimum canopy resistance, $F_1 - F_4$: weighting functions representing the effects of solar radiation, humidity, soil moisture and air temperature on plant stress, equations given by Chen and Dudhia (2001):

$$F_1 = \frac{r_s^{min}/r_s^{max} + f}{1 + f} \tag{42}$$

$$F_2 = \frac{1}{1 + h_s(e_s - e)} \tag{43}$$

$$F_3 = 1 - 0.0016(T_{ref} - T_a)^2 \tag{44}$$

$$F_4 = \sum_{i=1}^{N_{root}} \frac{(\theta_i - \theta_{wilt})d_i}{(\theta_{fc} - \theta_{wilt})d_t} \tag{45}$$

with r_s^{max}: maximum canopy resistance, $f = 0.55\frac{R_g}{R_{gl}}(\frac{2}{LAI})$, R_g: incident solar radiation, R_{gl}: minimum solar radiation needed for transpiration, h_s: parameter associated with water vapor deficit, $(e_s - e)$: water vapor deficit, T_{ref}: optimal temperature fro photosynthesis, T_a: air temperature, θ_i: soil moisture in soil layer i, θ_{fc}: soil moisture at field capacity, θ_{wilt}: soil moisture at wilting point, d_i: thickness of soil layer i, d_t: total thickness of soil, N_{root}: number of soil layers. Ershadi et al. (2015) recommend to use values for r_s^{min}, r_s^{max}, R_{gl}, h_s, T_{ref} given in lookup tables in Kumar et al. (2011). θ_{fc} and θ_{wilt} can be approximated using the 99th and the 1st percentile of the "after rain" soil moisture records constrained by the maximum or minimum values in the lookup table in Kumar et al. (2011) respectively (Ershadi et al., 2015).

Has to be calibrated for each crop, several times during the growth season (Rana and Katerji, 2000).

Model suggested by Rana et al. 1997: r_s is considered the sum of resistance due to plant architecture and stomatal regulation. It is expressed based on a relation between r_s and critical resistance r^* (Katerji et al., 1983):

$$r_s/r_a = f(r^*/r_a) \tag{46}$$

where r^* is calculated from meteorological parameters:

$$r^* = \frac{\lambda M}{R_{sp}T_a}\frac{\Delta + \gamma}{R_n - G}(T_a - T_d) \tag{47}$$

with M: molar weight of air, R_{sp}: specific gas constant for dry air, Δ: slope of saturation vapor pressure curve, T_a: air temperature, T_d: actual dew point temperature. The function f in eq. 46 varies with plant water status (measured predawn water potential), it is a linear function determined during calibration.

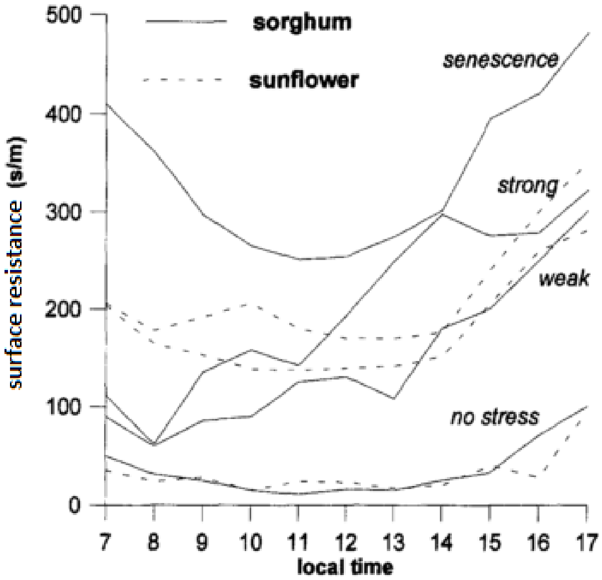

Figure 11: Hourly values of surface resistance r_s for two plant types and different water stress states obtained as the only unknown in the Penman-Monteith equation from measured ET by Rana et al. (1997)

5.1.2 Canopy resistance or bulk stomatal resistance

Parameter describing plant physiological resistance to evapotranspiration at the canopy level, mainly upscaled from leaf level stomatal resistance, e.g. in Shuttleworth and Wallace (1985) model: r_s^c is a function of LAI and mean stomatal resistance r_s^{st}:

$$r_s^c = \frac{r_s^{st}}{2LAI} \tag{48}$$

with r_s^{st}: mean stomatal resistance, expressed per unit surface area of vegetation, values for r_s^{st} are either estimated from literature recommendation (e.g. 400 $s\,m^{-1}$ by Shuttleworth and Wallace 1985), measured (high number of measurements needed in a short time (Rana and Katerji, 2000)) or calibrated from measured ET values.

Can also be determined with the Jarvis method (Described in Noilhan and Planton 1989) (Ershadi et al., 2015) or derived from remote sensing data (surface temperature and NDVI): Hope et al. (1986); Nemani and Running (1989), described in Kalma et al. (2008).

5.1.3 Stomatal resistance

parameter describing stomatal aperture at the leaf level; influences transpiration-driven water flux; stomatal aperture is sensitive to environmental influences such as soil moisture, light, air humidity, temperature, CO_2 concentration.

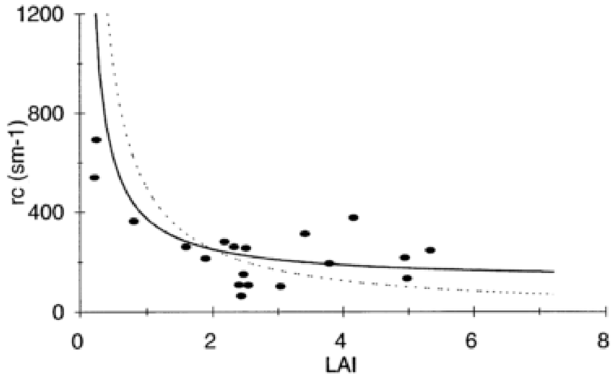

Figure 12: Dependence of canopy resistance r_s^c on LAI. r_s^c is calculated with two variations of eq. 48 using fixed values for mean stomatal resistance (dotted and full lines) and obtained experimentally from inverse modelling using measured evapotranspiration and simulated soil evaporation (Brisson et al., 1998).

Many models of stomatal conductance at the leaf level reviewed in Damour et al. (2010):

Empirical, multiplicative models of environmental influences Stomatal conductance g_s represented as the product of several environmental factors, e.g. in Jarvis (1976):

$$g_s = f_1(R_s) \cdot f_2(T) \cdot f_3(e_s - e) \cdot f_4(\psi_l) \tag{49}$$

with ψ_l: leaf water potential.

Major drawbacks / criticism: interaction between different factors are not considered; many parameters (e.g. Jarvis (1976): 10 parameters); empirical, new parameterization needed for changing conditions. Original Jarvis model doesn't include soil water stress, several of the models are only intended for conditions with no water limitations (Damour et al., 2010).

Limiting factor approach: g_s as a function of $g_{s,max}$ and the minimum among several response functions, e.g. Noe and Giersch (2004):

$$g_s = g_{s,max} \cdot min\left[f(R_s), f(e_s - e)\right] \tag{50}$$

Approaches with less parameters, less data demand: rough estimates of g_s from air humidity (Lohammar et al., 1980; Monteith, 1995) with only 1 or 2 parameters. Very simple but proven useful in non-extreme cases esp. no water stress (Damour et al., 2010).

Adaptations of Jarvis' model to include soil water stress (expressed as soil water deficit $\delta\theta$, pre-dawn water potential ψ_{pd} or sum of stress $S(\psi)$) by Stewart (1988); Misson et al. (2004); White et al. (1999)

Hydromechanical models describe the stomatal response to turgor pressure of guard cells, which is a function of water potential and osmotic pressure (e.g. Dewar (1995)). Detailed description of cell processes, plant physiology, drawback: Only theoretical use, high number of parameters (> 10 for some formulas), complex mathematical description, parameters difficult to estimate, observations not well simulated (Damour et al., 2010).

Adaptation to include soil water pressure: Dewar (2002) included a term based on abscisic acid concentration (see below); Gao et al. (2002) formulate a model where g_s is a function of water potential and osmotic pressure of the guard cells of the stomata (ψ_g and π_g).

Models relating g_s to photosynthesis rates One of the most commonly used models of g_s is Ball et al. (1987) that relates g_s to net photosynthesis rate A_{net}, relative humidity q_r and CO_2 concentration (mole fraction CO_2 at the leaf surface c_s):

$$g_s = C_{sl} A_{net} \frac{q_r}{c_s} \tag{51}$$

with $C_s l$: slope constant (empirical parameter).

Adaptations by Leuning (1990, 1995); Collatz et al. (1992); Soegaard et al. (1999). Advantage: relatively easy to use and parameterize (2-3 parameters). Disadvantage: No consideration of soil water status (Damour et al., 2010).

Adaptation of Ball's and Leuning's models to soil water stress: Introduction of parameters modifying the slope of the g_s A_{net} relationship (e.g. Tenhunen et al. (1990); Baldocchi (1997); Misson et al. (2004), these and more cited in Damour et al. (2010)).

Other models relate g_s to photosynthetic capacity (maximum rate of carbon fixation of a plant) (e.g. Farquhar et al. (1980); Farquhar and Wong (1984)) or to residual photosynthetic capacity ($A_{net} - A_{max}$, A_{max} is the maximum rate where CO_2 is not limiting), e.g. Jarvis and Davies (1998). Disadvantages: mismatches with observed values, complex to use: variables that are difficult to obtain are needed (Damour et al., 2010).

Models based on the control of abscisic acid (ABA) on g_s Abscisic acid (ABA) is a chemical signal transmitted to the leaf to indicate declining root and soil water potential. Some plant species (isohydric species) react to ABA by closing stomata, thus stopping transpiration and maintaining leaf water potential (ψ_l).

Modelling approaches: Tardieu and Davies (1993) represent g_s as a function of ABA concentration in the xylem and ψ_l. Gutschick and Simonneau (2002) included a function of ABA in the model of Ball et al. (1987).

Damour et al. (2010) advocate to also use H_2O_2 besides ABA.

Models based on hydraulic control on g_s Transpiration is represented as a flux (water transfer in the xylem) that is proportional to the difference in water potential of the leaf ψ_l and the soil ψ_s:

$$T = K_x(\psi_l - \psi_s) \tag{52}$$

with K_x: xylem hydraulic conductivity.

Applied by Oren et al. (1999); Tyree and Sperry (1988); Sperry et al. (1998); Jones and Sutherland (1991), different discretization of the plant (esp. K_x). Advantages: easy to understand, use and parameterize, disadvantages: focus on hydraulic mechanisms only, don't consider other controls.

other references: Zhao et al. (2016)

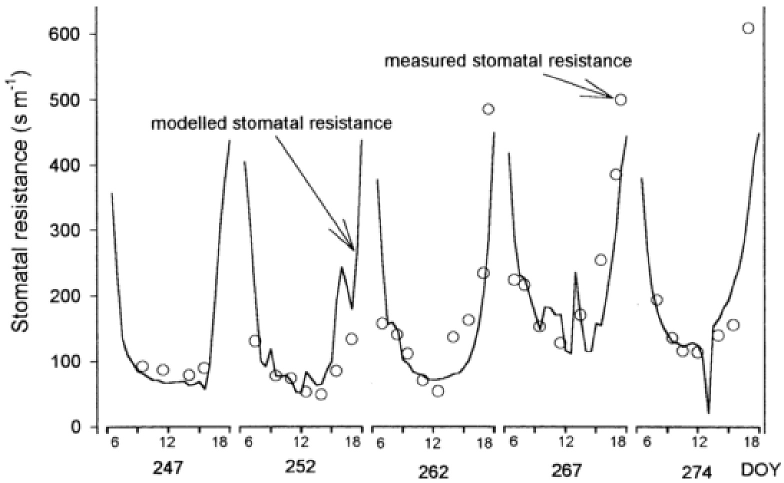

Figure 13: Stomatal resistance of tall, sparse millet modelled with the Ball and Berry model and measured with a leaf porometer for five consecutive days. The coefficient of determination is $R^2 = 0.78$. From Lund and Soegaard (2003).

5.1.4 Architectural resistance

Resistance of the xylem to water flow. Often neglected because it is assumed to be much smaller than stomatal resistance. Measured e.g. in Yang and Tyree (1994). Conductance of stem segments is proportional to stemdiameter $(2r)^{1.68}$. Architectural resistance of the trunk is $\approx$ 5 - 25 % of total resistance (trunk, crown and leaves); resistance of the trunk + crown is $\approx$ 35 - 50 % of total resistance for Acer saccharum and $\approx$ 45 - 65 % for Acer rubrum (two species of maple, Yang and Tyree (1994)).

5.1.5 Surface resistance of (bare) soil

Used in Shuttleworth and Wallace (1985) model, suggested values: 0 $s\,m^{-1}$ for fully saturated soils or free water surfaces to 2000 $s\,m^{-1}$ for fairly dry soils.

In H-TESSEL model calculated as a function of soil moisture θ and soil properties (Albergel et al., 2012) cited in Merlin et al. (2016):

$$r_s^s = \frac{\theta_{fc} - \theta_{res}}{\theta - \theta_{res}} \cdot r_{s,min}^s \quad for \quad \theta > \theta_{res} \tag{53}$$

with $r_{s,min}^s$: minimum soil surface resistance, set to 50 $s\,m^{-1}$, θ_{fc}: soil moisture at field capacity, θ_{res}: residual soil moisture.

In CLM model (empirical formula derived from Sellers et al. (1992), cited in Merlin et al. (2016)):

$$r_s^s = \exp(A - B\frac{\theta}{\theta_{fc}}) \tag{54}$$

with A and B: empirically derived parameters, given in Sellers et al. (1992) as 8.206 and 4.255.

In the Merlin et al. (2016) model: semi-empirical variation of Sellers' formula:

$$r_s^s = r_{s,ref}^s \exp(-\frac{\theta}{\theta_{efolding}}) \tag{55}$$

where the two parameters $r_{s,ref}^s$ and $\theta_{efolding}$ are estimated from a time series of soil evaporative efficiency SEE (ratio of actual soil evaporation to potential evaporation) and soil moisture θ.

Empirical formula proposed by Dolman (1993):

$$r_s^s = a\theta^b \tag{56}$$

with a and b: empirical constants, recommended values: $a = 3.5 s\,m^{-1}$ and $b = -2.3$, θ: surface layer soil moisture.

Several methods for calculation r_s^s as a function of soil moisture reviewed in Mahfouf and Noilhan (1991), linear models of the form $r_s^s = m\theta + c$ with parameters m and c depending on potential evaporation in Daamen and Simmonds (1996).

Calculated from inverse modelling using the formula proposed by Shuttleworth and Wallace (1985) solved for r_s^s. Soil evaporation ET_s can be obtained from measurements or calculated as the difference between measured evapotranspiration and transpiration (e.g. Lund and Soegaard 2003):

$$r_s^s = \left[\left(\frac{\Delta(R_n - G) + (\rho c_p D / r_a^s)}{\lambda ET_s} - \Delta\right) / \gamma - 1\right] r_a^s \tag{57}$$

Alternatively, potential soil evaporation can be calculated assuming that r_s^s is 0, and then compared to (measured or modelled) actual evaporation (Daamen and Simmonds, 1996):

$$r_s^s = \frac{\Delta + \gamma}{\gamma}(\frac{E_{pot}}{E_{act}} - 1)r_a \tag{58}$$

both of these approaches are very sensitive to measured (or otherwisely modeled) evaporation and r_a.

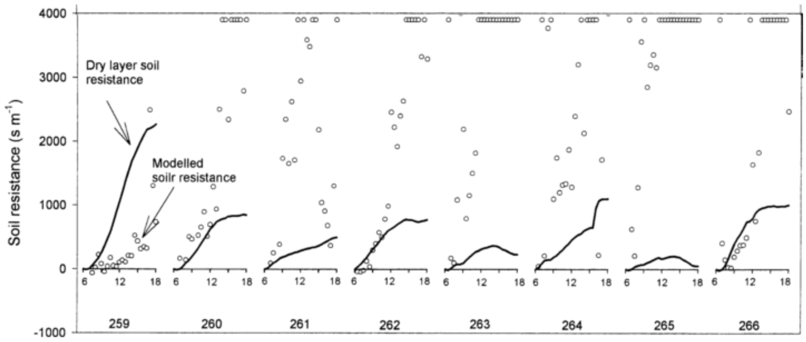

Figure 14: Development of soil surface resistance (calculated from inverse modelling with the Shuttleworth-Wallace formula and measured ET and transpiration) over the course of drying period of five consecutive days. Values of $\approx 0 sm^{-1}$ in the morning indicate rewetting of the topmost soil layer during the night (Lund and Soegaard, 2003).

5.2 Aerodynamic resistance

Determined by the wind speed profile (assumed to be logarithmic or following a power law) and surface characteristics.

5.2.1 Single aerodynamic resistance r_a

As in big leaf approach of the Penman-monteith model, e.g. calculated with the following equation given by Thom (1975):

$$r_a = \frac{1}{k^2 u} \left[\ln(\frac{z-d}{z_{0m}}) \ln(\frac{z-d}{z_{0v}}) \right] \tag{59}$$

where $k = 0.41$: von Karman's constant, u: wind speed, z: measurement height, d: displacement height, z_{0m} and z_{0v}: roughness heights form momentum and water vapor transfer.

Roughness parameters d, z_{0m} and z_{0v} can either be calculated as functions of canopy height h_c: $d = 0.66 h_c$, $z_{0m} = 0.1 h_c$ and $z_{0v} = 0.01 h_c$ as recommended by Brutsaert (2005) or can be estimated via a physically-based method such as the one by Su et al. (2001) (Ershadi et al., 2015).

Rana and Katerji (1998) use a formula given by Tolk et al. (1995), who in turn cite Thom (1975), also given by Verma (1989), that is actually a formula for aerodynamic resistance to heat transfer r_{ah}:

$$r_{ah} = \rho c_p \frac{T_s - T_a}{H} \tag{60}$$

where surface and air temperature T_s and T_a and sensible heat flux H are measured directly, the latter with eddy correlation and Bowen ratio measurement systems. Disadvantages: measurements of H neccessary, the assumption that $r_{ah} = r_a$ is not explicitly mentioned in Tolk et al. (1995), implications of this assumption are not discussed.

Similar formula to the one proposed by Thom (1975) that accounts for the dependance of r_a on atmospheric buoyancy (and also assumes that $r_a = r_{ah}$) given by Choudhury and Monteith (1988):

$$r_a = \frac{(\ln](z_u - d)/z_{0v}])^2}{k^2 u}(1+\delta)^{\epsilon} \tag{61}$$

with

$$\delta = 5g(z_u - d)(T_s - T_a)/(T_a u^2) \tag{62}$$

and $\epsilon = -2$ if $\delta < 0$, otherwise $\epsilon = -0.75$, where g is gravitational acceleration.

5.2.2 Above the canopy r_a^a

In the original Shuttleworth-Wallace model:

r_a^a differs with LAI between values for full vegetation cover ($LAI > 4$, $r_a^a(\alpha)$) and values for bare soil ($LAI = 0$, $r_a^a(0)$):

$$r_a^a = \frac{1}{4} LAI \cdot r_a^a(\alpha) + \frac{1}{4}(4 - LAI) \cdot r_a^a(0) \tag{63}$$

$r_a^a(\alpha)$ and $r_a^a(0)$ are calculated as:

$$r_a^a(\alpha) = \frac{ln(\frac{z_m - d}{z_{om}} + \phi_M) ln(\frac{z_h - d}{z_{oh}} + \phi_H)}{k^2 u(z_m)} \tag{64}$$

$$r_a^a(0) = \frac{(ln\frac{z_m}{z_{om}} + \phi_M)(ln\frac{z_h}{z_{oh}} + \phi_H)}{k^2 u(z_m)} - r_a^s(0) \tag{65}$$

with z_h: height of humidity measurement, ϕ_M: atmospheric diabatic correction factor (Lu et al. (2014) refer to Brutsaert (1982)), ϕ_H: atmospheric diabatic correction factor for heat.

Formula suggested by Shuttleworth and Gurney (1990):

$$r_a^a = \frac{1}{k\,u} \ln(\frac{z-d}{h_c - d}) + \frac{h_c}{nK_h}\left\{\exp\left[n(1 - \frac{z_{0m}+d}{h_c})\right] - 1\right\} \tag{66}$$

Abbreviations as above, K_h: eddy diffusion coefficient at the top of canopy, calculated as $K_h = k\,u_*(h_c - d)$ with friction velocity $u_* = k\,u/\ln[(z-d)/z_{0m}]$, n: eddy diffusivity decay constant, values given by Zhou et al. (2006), recommended by Ershadi et al. (2015); Brutsaert (1982); Gao et al. (2016):

$$n = \begin{cases} 2.5 \quad for \quad h_c \leq 1 \\ 2.306 + 0.19 h_c \quad for \quad 1 < h_c < 10 \\ 4.25 \quad for \quad h_c \geq 10 \end{cases} \tag{67}$$

with h_c: vegetation height.

5.2.3 Between the canopy and mean surface flow height r_a^c

In Shuttleworth and Wallace (1985) model: r_a^c also a function of LAI:

$$r_a^c = \frac{r_b \sigma_b}{2LAI} \tag{68}$$

with σ_b: shielding factor, equal to 0.5; r_b: mean boundary layer resistance, also expressed per unit surface area of vegetation, in the order of 25 - 50 $s\,m^{-1}$, much smaller than stomatal resistance, less important (Shuttleworth and Wallace, 1985; Brisson et al., 1998). r_b can also be calculated according to Shuttleworth and Gurney (1990) (cited in Gao et al. 2016):

$$r_b = \frac{100}{n} \frac{\sqrt{w/u_h}}{1 - \exp(-n/2)} \tag{69}$$

with w: representative leaf width, u_h: wind speed at the top of the canopy.

In high, sparse crops such as millet, Lund and Soegaard (2003) distinguish between r_a^c forced by momentum and free r_a^c: In the former case they use the equation proposed by Jones (2013):

$$r_a^c = 151\sqrt{\frac{w}{u}} \tag{70}$$

with w: leaf width and u: wind speed at reference height.

In the latter case, they use the equation proposed by Brenner and Jarvis (1995):

$$r_a^c = 0.93\sqrt[4]{\frac{wv}{D_h^3 g a_t (T_l - T_a)}} \tag{71}$$

with v: kinematic viscosity, D_h: diffusivity of heat, g: gravitational acceleration, a_t: coefficient of thermal expansion in air, T_l and T_a: leaf and air temperature.

5.2.4 Between the soil surface and mean surface flow height r_a^s

In the original Shuttleworth-Wallace model:

r_a^s differs with LAI between values for full vegetation cover ($LAI > 4$) ($r_a^s(\alpha)$ and values for bare soil ($LAI = 0$) ($r_a^s(0)$:

$$r_a^s = \frac{1}{4} LAI \cdot r_a^s(\alpha) + \frac{1}{4}(4 - LAI) \cdot r_a^s(0) \tag{72}$$

$r_a^s(\alpha)$ is calculated as:

$$r_a^s(\alpha) = \int_0^{d+z_{om}} \frac{dz}{K(z)} = \frac{ln\frac{z-d}{z_{om}} + \phi_M}{k^2 u(z)} \frac{h_c}{n(h\_d)} \{exp\, n - exp[n(1 - \frac{d+z_m}{h_c})]\} \tag{73}$$

with d: zero plane displacement height, calculated as $d = 0.63h_c$ with h_c being crop height (Monteith, 1965), z_{om}: crop roughness length, calculated as $z_0 = 0.13h_c$, $K(z)$: eddy diffusion coefficient at height z, ϕ_M: atmospheric diabatic correction factor, k: von Karman's constant ($= 0.41$), $u(z)$: wind speed at height z, n: extinction coefficient of the eddy diffusion, derived from linear interpolation between 2.5 for $h_c = 1m$ and 4.25 for $h_c > 10m$, z_m: height of wind measurement.

$r_a^s(0)$ is calculated as:

$$r_a^s(0) = \frac{(ln\frac{h_c}{z_{om}} + \phi_M)(ln\frac{h_c}{z_{oh}} + \phi_H)}{k^2 u(h_c)} \tag{74}$$

with z_{oh}: roughness length of bare soil governing heat transfer and ϕ_H: atmospheric diabatic correction factor for heat.

Formula suggested by Shuttleworth and Gurney (1990):

$$r_a^s = \frac{h_c \exp(n)}{n\, K_h} \left\{ \exp(-\frac{n\, z'_{0m}}{h_c}) - \exp\left[-n(\frac{z_{0m+d}}{h_c})\right] \right\} \tag{75}$$

with z'_{0m}: roughness length of bare soil surface, assumed to be 0.01 m by van Bavel and Hillel (1976).

6 Arid and semi-arid regions

Evaporation is an important part of the water balance, (semi-) arid regions characterized by water scarcity, need for irrigation, problems caused by salinization (Rana and Katerji, 2000). A negative correlation between ET rates and water table depth is generally observed (Cooper et al., 2006). Mediterranean landscapes usually very patchy, not homogeneous.

High range of evapotranspiration values and weather variables, dependant on water regime, differences between dry and wet seasons, winter and summer, day and night (Rana and Katerji, 2000).

"ET measurement methods are based on concepts that can be critical under semi-arid and arid environments for several reasons: representativeness (the weighing lysimeter, for example); (ii) instrumentation (air humidity sensors for example); (iii) microclimate (advection regime); and (iv) hypothesis of applicability (the simplified aerodynamic method for example)." (Rana and Katerji, 2000).

Transpiration important part of total Evapotranspiration, big leaf approach not appropriate;
Oudin et al. (2005): In arid catchments, unlike in others, model performance is improved by using temporally resolved data instead of daily mean data.

Reference evapotranspiration method not recommended (Mata-González et al. 2005, see sec. 3.7).

Formulas for the calculation of stomatal resistance / conductance should include water stress (Damour et al., 2010).

Strong heterogeneity in water availability (esp. caused by irrigation) lead to discontinuity in water vapor concentrations at surface level. This violates the requirement of all measurement and modelling methods that the profiles of air temperature, water vapor concentration and windspeed are constant along the horizontal axis. This can lead to advective effects (observed by e.g. Prueger et al. 1996) that cause considerable errors (Rana and Katerji, 2000).

Several empirical formulas unsuitable in non-irrigated (semi-)arid ares: Makkink formula (developed for grasslands in the netherlands), Jensen-Haise (for irrigated areas only), Thornthwaite (developed in valley with sufficient water supply, widely misused in semi-arid areas), Linacre (also for well water surfaces), Haude (for Germany).

Probably suitable: McGuinnes and Bordne (Developed in Florida) Hargreaves (Davies, California), Blainey & Criddle, Kharrufa, Oudin.

Case studies in (semi-) arid regions: Dugas et al. (1991); Stannard (1993); Prueger et al. (1996); Steduto et al. (1997); Brisson et al. (1998); Mastrorilli et al. (1998); Rana and Katerji (1998); Dahm et al. (2002); Yepez et al. (2003); Cooper et al. (2006); Tang et al. (2010); Githui et al. (2012); Shadmani et al. (2012); Bohn and Vivoni (2015); Ershadi et al. (2015); Allam et al. (2016); Campos et al. (2016); El-shirbeny et al. (2016); Gao et al. (2016); Li et al. (2016); Wu (2016).

References

Albergel, C., Balsamo, G., De Rosnay, P., Mu??oz-Sabater, J., and Boussetta, S. (2012). A bare ground evaporation revision in the ECMWF land-surface scheme: Evaluation of its impact using ground soil moisture and satellite microwave data. *Hydrology and Earth System Sciences*, 16(10):3607–3620.

Allam, M. M., Jain Figueroa, A., McLaughlin, D. B., and Eltahir, E. A. B. (2016). Estimation of evaporation over the Upper Blue Nile basin by combining observations from satellites and river flow gauges. *Water Resources Research*, pages n/a—-n/a.

Allen, R. G., Pereira, L. S., Raes, D., and Smith, M. (1998). Crop evapotranspiration – guidelines for computing crop water requirements. In *Irrigation and Drainage Paper No. 56*. Food and Agriculture Organization of the United Nations.

Allen, R. G., Pruitt, W. O., Wright, J. L., Howell, T. A., Ventura, F., Snyder, R., Itenfisu, D., Steduto, P., Berengena, J., Yrisarry, J. B., Smith, M., Pereira, L. S., Raes, D., Perrier, A., Alves, I., Walter, I., and Elliott, R. (2006). A recommendation on standardized surface resistance for hourly calculation of reference ETo by the FAO56 Penman-Monteith method. *Agricultural Water Management*, 81(1-2):1–22.

Allen, R. G., Tasumi, M., Morse, A., Trezza, R., Wright, J. L., Bastiaanssen, W., Kramber, W., Lorite, I., Robison, C. W., Morse, A., Trezza, R., Wright, J. L., Bastiaanssen, W., Kramber, W., Lorite, I., Robison, C. W., Morse, A., Trezza, R., Wright, J. L., Bastiaanssen, W., Kramber, W., Lorite, I., and Robison, C. W. (2007a). Satellite-Based Energy Balance for Mapping Evapotranspiration with Internalized Calibration (METRIC)Applications. *Journal of Irrigation and Drainage Engineering*, 133(4):395–406.

Allen, R. G., Tasumi, M., Morse, A., Trezza, R., Wright, J. L., Bastiaanssen, W., Kramber, W., Lorite, I., Robison, C. W., Morse, A., Trezza, R., Wright, J. L., Bastiaanssen, W., Kramber, W., Lorite, I., Robison, C. W., Morse, A., Trezza, R., Wright, J. L., Bastiaanssen, W., Kramber, W., Lorite, I., and Robison, C. W. (2007b). Satellite-Based Energy Balance for Mapping Evapotranspiration with Internalized Calibration (METRIC)Applications. *Journal of Irrigation and Drainage Engineering*, 133(4):395–406.

Anderson, M. C. (1997). A Two-Source Time-Integrated Model for Estimating Surface Fluxes Using Thermal Infrared Remote Sensing. *Remote Sensing of Environment*, 60(2):195–216.

Anderson, M. C., Kustas, W. P., and Norman, J. M. (2007a). Upscaling flux observations from local to continental scales using thermal remote sensing. *Agronomy Journal*, 99(1):240–254.

Anderson, M. C., Norman, J. M., Mecikalski, J. R., Otkin, J. A., and Kustas, W. P. (2007b). A climatological study of evapotranspiration and moisture stress across the continental United States based on thermal remote sensing: 1. Model formulation. *Journal of Geophysical Research Atmospheres*, 112(10):1–17.

Andreas, E. L. (1989). Two-Wavelength Method of Measuring Path-Averaged Turbulent Surface Heat Fluxes.

Andréassian, V., Perrin, C., and Michel, C. (2004). Impact of imperfect potential evapotranspiration knowledge on the efficiency and parameters of watershed models. *Journal of Hydrology*, 286(1-4):19–35.

Ashktorab, H., Pruitt, W. O., Pawu, K. T., and George, W. V. (1989). Energy-Balance Determinations Close To the Soil Surface Using a Micro-Bowen Ration System. *Agricultural and Forest Meteorology*, 46(3):259–274.

Aubinet, M., Vesala, T., and Papale, D. (2012). *Eddy Covariance*. Springer Science+Business Media.

Baier, W. and Robertson, W. (1966). A new versatile soil moisture. *Canadian Journal of Plant Science*, 46:299–315.

Baldocchi, D. (1997). Measuring and modelling carbon dioxide and water vapour exchange over a temperate broad-leaved forest during the 1995 summer drought. *Plant Cell and Environment*, 20(9):1108–1122.

Baldocchi, D., Falge, E., Gu, L. H., Olson, R., Hollinger, D., Running, S., Anthoni, P., Bernhofer, C., Davis, K., Evans, R., Fuentes, J., Goldstein, A., Katul, G., Law, B., Lee, X. H., Malhi, Y., Meyers, T., Munger, W., Oechel, W., U, K. T. P., Pilegaard, K., Schmid, H. P., Valentini, R., Verma, S., Vesala, T., Wilson, K., Wofsy, S., Paw, U. K. T., Pilegaard, K., Schmid, H. P., Valentini, R., Verma, S., Vesala, T., Wilson, K., and Wofsy, S. (2001). FLUXNET: A New Tool to Study the Temporal and Spatial Variability of Ecosystem-Scale Carbon Dioxide, Water Vapor, and Energy Flux Densities. *Bulletin of the American Meteorological Society*, 82(11):2415–2434.

Baldocchi, D. D., Luxmoore, R. J., and Hatfield, J. L. (1991). Discerning the forest from the trees: an essay on scaling canopy stomatal conductance. *Agricultural and Forest Meteorology*, 54(2-4):197–226.

Ball, J., Woodrow, I., and Berry, J. (1987). A Model Predicting Stomatal Conductance and its Contribution to the Control of Photosynthesis under Different Environmental Conditions. In Biggins, J., editor, *Progress in Photosynthesis Research*, pages 221–224. Springer Netherlands.

Ball, M. C., Cowan, I. R., and Farquhar, G. D. (1988). Maintenance of Leaf Temperature and the Optimization of Carbon Gain in Relation to Water-Loss in a Tropical Mangrove Forest. *Australian Journal of Plant Physiology*, 15(1-2):263–276.

Bastiaanssen, W. G. M., Menenti, M., Feddes, R. A., and Holtslag, A. A. M. (1998). A remote sensing surface energy balance algorithm for land (SEBAL): 1. Formulation. *Journal of Hydrology*, 212-213(1-4):198–212.

Beven, K. (1979). A sensitivity analysis of the Penman-Monteith actual evapotranspiration estimates. *Journal of Hydrology*, 44(3-4):169–190.

Blaney, H. F. and Criddle, W. D. (1950). Determining water requirements in irrigated areas from climatological and irrigation data. Technical report, United States Geological Survey Soil Conservation Service, Washington.

Bohn, T. J. and Vivoni, E. R. (2015). Process-based characterization of evapotranspiration sources over the North American monsoon region. *Water Resources Research*, pages n/a—-n/a.

Bouchet, R. J. (1963). Evapotranspiration reelle, evapotranspiration potentielle, et production agricole. *Annales agronomiques*, 14(5):743–824.

Bowen, I. S. (1926). The Ratio of Heat Losses by Conduction and by Evaporation from any Water Surface. *Physical Review*, 27(6):779–787.

Brenner, A. J. and Incoll, L. D. (1997). The effect of clumping and stomatal response on evaporation from sparsely vegetated shrublands. *Agricultural and Forest Meteorology*, 84(34):187–205.

Brenner, A. J. and Jarvis, P. G. (1995). A heated leaf replica technique for determination of leaf boundary layer conductance in the field. *Agricultural and Forest Meteorology*, 72(3-4):261–275.

Brisson, N., Itier, B., L'Hotel, J. C., and Lorendeau, J. Y. (1998). Parameterisation of the Shuttleworth-Wallace model to estimate daily maximum transpiration for use in crop models. *Ecological Modelling*, 107(23):159–169.

Brutsaert, W. (1982). *Evaporation into the Atmosphere. Theory, History and Applications.* Springer, Dordrecht.

Brutsaert, W. (2005). *Hydrology. An Introduction.* Cambridge University Press, Cambridge.

Burgess, S. S., Adams, M. a., Turner, N. C., Beverly, C. R., Ong, C. K., Khan, a. a., and Bleby, T. M. (2001). An improved heat pulse method to measure low and reverse rates of sap flow in woody plants. *Tree physiology*, 21(9):589–598.

Campos, I., González-Piqueras, J., Carrara, A., Villodre, J., and Calera, A. (2016). Estimation of total available water in the soil layer by integrating actual evapotranspiration data in a remote sensing-driven soil water balance. *Journal of Hydrology*, 534:427–439.

Carlson, T. N., Capehart, W. J., and Gillies, R. R. (1995). A New Look at the Simplified Method for Remote Sensing of Daily Evapotranspiration. *Remote Sensing of Environment*, 54:161 – 167.

Chen, F. and Dudhia, J. (2001). Coupling an Advanced Land SurfaceHydrology Model with the Penn StateNCAR MM5 Modeling System. Part I: Model Implementation and Sensitivity. *Monthly Weather Review*, 129(4):569–585.

Choudhury, B. J. and Monteith, J. L. (1988). A four-layer model for the heat budget of homogeneous land surfaces. *Quarterly Journal of the Royal Meteorological Society*, 114(480):373–398.

Collatz, G. J., Ribas-Carbo, M., and Berry, J. A. (1992). Coupled photosynthesis-stomatal conductance model for leaves of c4 plants. *Australian Journal of Plant Physiology*, 19(5):519 – 538.

Conradt, T., Wechsung, F., and Bronstert, A. (2013). Three perceptions of the evapotranspiration landscape: comparing spatial patterns from a distributed hydrological model, remotely sensed surface temperatures, and sub-basin water balances. *Hydrology and Earth System Sciences*, 17(7):2947–2966.

Cooper, D. J., Sanderson, J. S., Stannard, D. I., and Groeneveld, D. P. (2006). Effects of long-term water table drawdown on evapotranspiration and vegetation in an arid region phreatophyte community. *Journal of Hydrology*, 325(1-4):21–34.

Daamen, C. and Simmonds, L. (1994). Soil Water, Energy And Transpiration. A numerical model of water and energy fluxes in soil profiles and sparse canopies. Technical report, Natural Resources Institute, Reading.

Daamen, C. C. and Simmonds, L. P. (1996). Measurement of evaporation from bare soil and its estimation using surface resistance. *Water Resources Research*, 32(5):1393–1402.

Daamen, C. C., Simmonds, L. P., Wallace, J. S., Laryea, K. B., and Sivakumar, M. V. K. (1993). Use of microlysimeters to measure evaporation from sandy soils. *Agricultural and Forest Meteorology*, 65:159–173.

Dahm, C. N., Cleverly, J. R., Allred Coonrod, J. E., Thibault, J. R., Mcdonnell, D. E., and Gilroy, D. J. (2002). Evapotranspiration at the land/water interface in a semi-arid drainage basin. *Freshwater Biology*, 47(4):831–843.

Dalton, J. (1802). Experimental essays on the constitution of mixed gases: on the force of steam or vapor from water or other liquids in different temperatures, both in a Torricelli vacuum and in air; on evaporation; and on expansion of gases by heat. *Memoirs and proceedings of the Manchester Literary & Philosophical Society*, 5:536 – 602.

Damour, G., Simonneau, T., Cochard, H., and Urban, L. (2010). An overview of models of stomatal conductance at the leaf level. *Plant, Cell and Environment*, 33(9):1419–1438.

Dawson, T., Mambelli, S., Plamboeck, A., Templer, P., and Tu, K. (2002). Stable Isotopes in Plant Ecology. *Annual Review of Ecology and Systematics*, 33(1):507–559.

De Jong, R. and Bootsma, A. (1996). Review of recent developments in soil water simulation models. *Revue des developpements recents dans les modeles simulant l'eau du sol*, 76(3):263–273.

Denmead, O. T., Dunin, F. X., Leuning, R., and Raupach, M. R. (1996). Measuring and modelling soil evaporation in wheat crops. *Physics and Chemistry of the Earth*, 21(3):97–100.

Denmead, O. T., Dunin, F. X., Wong, S. C., and Greenwood, E. A. N. (1993). Measuring water use efficiency of Eucalypt trees with chambers and micrometeorological techniques. *Journal of Hydrology*, 150(2-4):649–664.

Dewar, R. C. (1995). Interpretation of an Empirical-Model for Stomatal Conductance in Terms of Guard-Cell Function. *Plant Cell and Environment*, 18(4):365–372.

Dewar, R. C. (2002). The Ball-Berry-Leuning and Tardieu-Davies stomatal models: Synthesis and extension within a spatially aggregated picture of guard cell function. *Plant, Cell and Environment*, 25(11):1383–1398.

Dolman, A. J. (1993). A multiple-source land surface energy balance model for use in general circulation models. *Agricultural and Forest Meteorology*, 65(1-2):21–45.

Domec, J. C., Sun, G., Noormets, A., Gavazzi, M. J., Treasure, E. A., Cohen, E., Swenson, J. J., McNulty, S. G., and King, J. S. (2012). A comparison of three methods to estimate evapotranspiration in two contrasting loblolly pine plantations: Age-related changes in water use and drought sensitivity of evapotranspiration components. *Forest Science*, 58(5):497–512.

Doorenbos, J. and Pruitt, W. O. (1977). Crop water requirements. In *Irrigation and Drainage Paper No. 24*. Food and Agriculture Organization of the United Nations.

Dugas, W. A., Fritschen, L. J., Gay, L. W., Held, A. A., Matthias, A. D., Reicosky, D. C., Steduto, P., and Steiner, J. L. (1991). Bowen ratio, eddy correlation, and portable chamber measurements of sensible and latent heat flux over irrigated spring wheat. *Agricultural and Forest Meteorology*, 56(1-2):1–20.

Dyck, S. and Peschke, G. (1995). *Grundlagen der Hydrologie*. Verlag für Bauwesen, Berlin, 3 edition.

El-shirbeny, M. A., Abdellatif, B., Ali, A.-e. M., and Saleh, N. H. (2016). Evaluation of Hargreaves Based on Remote Sensing Method To Estimate Potential Crop Evapotranspiration. 11(23):2143–2149.

Ershadi, A., McCabe, M. F., Evans, J. P., and Wood, E. F. (2015). Impact of model structure and parameterization on PenmanMonteith type evaporation models. *Journal of Hydrology*, 525:521–535.

Farquhar, G. and Wong, S. (1984). An Empirical Model of Stomatal Conductance. *Australian Journal of Plant Physiology*, 11(3):191 – 210.

Farquhar, G. D., von Caemmerer, S., and Berry, J. A. (1980). A biochemical model of photosynthetic CO2 assimilation in leaves of C3 species. *Planta*, 149(1):78–90.

Finnigan, J. J., Clement, R., Malhi, Y., Leuning, R., and Cleugh, H. A. (2003). Re-evaluation of long-term flux measurement techniques. Part I: Averaging and coordinate rotation. *Boundary-Layer Meteorology*, 107(1):1–48.

Foken, T. and Wichura, B. (1996). Tools for quality assessment of surface-based flux measurements. *Agricultural and Forest Meteorology*, 78:83 – 105.

Gao, G., Zhang, X., and Yu, T. (2016). Evapotranspiration of a Populus euphratica forest during the growing season in an extremely arid region of northwest China using the ShuttleworthWallace model. *Journal of Forestry Research*, 27(4):879–887.

Gao, Q., Zhao, P., Zeng, X., Cai, X., and Shen, W. (2002). A model of stomatal conductance to quantify the relationship between leaf transpiration, microclimate and soil water stress. *Plant, Cell & Environment*, 25:1373–1381.

Gasca-Tucker, D. L., Acreman, M. C., Agnew, C. T., and Thompson, J. R. (2007). Estimating evaporation from a wet grassland. *Hydrology and Earth System Sciences Discussions*, 11(1):270–282.

Githui, F., Selle, B., and Thayalakumaran, T. (2012). Recharge estimation using remotely sensed evapotranspiration in an irrigated catchment in southeast Australia. *Hydrological Processes*, 26(9):1379–1389.

Glenn, E. P., Huete, A. R., Nagler, P. L., Hirschboeck, K. K., and Brown, P. (2007). Integrating Remote Sensing and Ground Methods to Estimate Evapotranspiration. *Critical Reviews in Plant Sciences*, 26(3):139–168.

Griffis, T. J. (2013). Tracing the flow of carbon dioxide and water vapor between the biosphere and atmosphere: A review of optical isotope techniques and their application. *Agricultural and Forest Meteorology*, 174-175(August):85–109.

Grime, V. L. and Sinclair, F. L. (1999). Sources of error in stem heat balance sap flow measurements. *Agricultural and Forest Meteorology*, 94(2):103–121.

Guo, D., Westra, S., and Maier, H. R. (2016). An R package for modelling actual, potential and reference evapotranspiration. *Environmental Modelling & Software*, 78:216–224.

Gutschick, V. P. and Simonneau, T. (2002). Modelling stomatal conductanceof field-grown sunflower under varying soil water content and leafenvironment: comparison of three models of stomatal response toleaf environment and coupling with an abscisic acid-based modelof stomatal response to soil dryi. *Plant, Cell & Environment*, 25(11):1423–1434.

Guyot, A., Cohard, J. M., Anquetin, S., and Galle, S. (2012). Long-term observations of turbulent fluxes over heterogeneous vegetation using scintillometry and additional observations: A contribution to AMMA under Sudano-Sahelian climate. *Agricultural and Forest Meteorology*, 154-155:84–98.

Guyot, A., Cohard, J. M., Anquetin, S., Galle, S., and Lloyd, C. R. (2009). Combined analysis of energy and water balances to estimate latent heat flux of a sudanian small catchment. *Journal of Hydrology*, 375(1-2):227–240.

Hamon, W. R. (1960). *Estimating potential evapotranspiration.* B.sc. thesis, Massachusetts Institute of Technology.

Hargreaves, G. H. (1975). Moisture availability and crop production. *American Society of Agricultural and Biological Engineers*, 18(5):980 – 984.

Hargreaves, G. H. and Samani, Z. A. (1982). Estimating Potential Evapotranspiration. *Journal of the Irrigation and Drainage Division*, 108(3):225–230.

Hargreaves, G. H. and Samani, Z. A. (1985). Reference Crop Evapotranspiration from Temperature. *Applied engineering in agriculture*, 1(2):96 – 99.

Heitman, J. L., Horton, R., Sauer, T. J., and DeSutter, T. M. (2008a). Sensible heat observations reveal soil-water evaporation dynamics. *Journal of Hydrometeorology*, 9:165–171.

Heitman, J. L., Xiao, X., Horton, R., and Sauer, T. J. (2008b). Sensible heat measurements indicating depth and magnitude of subsurface soil water evaporation. *Water Resources Research*, 44:1–7.

Hipps, L. E. and Zehr, D. F. (1995). Determination of evaporation from integrated profiles of humidity and temperature over an inhomogeneous surface. *Boundary-Layer Meteorology*, 75(3):287–299.

Holland, S., Heitman, J. L., Howard, A., Sauer, T. J., Giese, W., Ben-Gal, A., Agam, N., Kool, D., and Havlin, J. (2013). Micro-Bowen ratio system for measuring evapotranspiration in a vineyard interrow. *Agricultural and Forest Meteorology*, 177:93–100.

Hope, A. S., Petzold, D. E., Goward, S. N., and Ragan, R. M. (1986). Simulated relationships between spectral reflectance, thermal emissions, and evapotranspiration of a soybean canopy. *Water Resources Bulletin*, 22(6):1011–1019.

Horita, J., Rozanski, K., and Cohen, S. (2008). Isotope effects in the evaporation of water: a status report of the Craig-Gordon model. *Isotopes in environmental and health studies*, 44(1):23–49.

Iritz, Z., Lindroth, A., and Gärdenäs, A. (1997). Open ventilated chamber system for measurements of H2O and CO2 fluxes from the soil surface. *Soil Technology*, 10(3):169–184.

Jarvis, A. and Davies, W. (1998). The coupled response of stomatal conductance to photosynthesis and transpiration. *Journal of Experimental Botany*, 49(March):399–406.

Jarvis, P. G. (1976). The Interpretation of the Variations in Leaf Water Potential and Stomatal Conductance Found in Canopies in the Field. *Philosophical Transactions of the Royal Society of London B: Biological Sciences*, 273(927):593–610.

Jensen, M. E. and Haise, H. R. (1965). Estimating evapotranspiration from solar radiation. *Journal of Irrigation and Drainage Division1*, 89:15–41.

Jhorar, R. K., Smit, A. A. M. F. R., Bastiaanssen, W. G. M., and Roest, C. W. J. (2011). Calibration of a distributed irrigation water management model using remotely sensed evapotranspiration rates and groundwater heads. *Irrigation and Drainage*, 60:57 – 69.

Jones, H. G. (2013). *Plants and microclimate. A quantitative approach to environmental plant physiology.* Cambridge University Press, Cambridge.

Jones, H. G. and Sutherland, R. A. (1991). Stomatal control of xylem embolism. *Plant, Cell and Environment*, 14(6):607–612.

Kalma, J. D., McVicar, T. R., and McCabe, M. F. (2008). Estimating land surface evaporation: A review of methods using remotely sensed surface temperature data. *Surveys in Geophysics*, 29(4-5):421–469.

Katerji, N., Perrier, A., Renard, D., and Oulid Aissa, A. K. (1983). Modélisation de l'évapotranspiration réelle ETR d'une parcelle de luzerne : rôle d'un coefficient cultural. *Agronomie*, 3(6):513 – 521.

Kharrufa, N. S. (1985). Simplified equation for evapotranspiration in arid regions. *Beiträge zur Hydrologie*, 5(1):39 – 47.

Kjelgaard, J., Stockle, C., Black, R., and Campbell, G. (1997). Measuring sap flow with the heat balance approach using constant and variable heat inputs. *Agricultural and Forest Meteorology*, 85(3-4):239–250.

Kool, D., Agam, N., Lazarovitch, N., Heitman, J. L., Sauer, T. J., and Ben-gal, A. (2014). A review of approaches for evapotranspiration partitioning. *Agricultural and Forest Meteorology*, 184:56–70.

Kumar, A., Chen, F., Niyogi, D., Alfieri, J. G., Ek, M., and Mitchell, K. (2011). Evaluation of a Photosynthesis-Based Canopy Resistance Formulation in the Noah Land-Surface Model. *Boundary-Layer Meteorology*, 138(2):263–284.

Lascano, R., Van Bavel, C., Hatfield, J., and Upchurch, D. (1987). Energy and water balance of a sparse crop: simulated and measured soil and crop evaporation. *Soil Science Society of America Journal*, 51:1113–1121.

Leenhardt, D., Voltz, M., and Rambal, S. (1995). A survey of several agroclimatic soil water balance models with reference to their spatial application.pdf. *European Journal of Agronomy*, 4(1):1–14.

Leuning, R. (1990). Modelling Stomatal Behaviour and and Photosynthesis of Eucalyptus grandis. *Australian Journal of Plant Physiology1*, 17(2):159 – 175.

Leuning, R. (1995). A critical appraisal of a combined stomatal-photosynthesis model for C3 plants.

Lewis, J. M. (1995). The story behind the Bowen ratio. *Bulletin of the American Meteorological Society*, 76(12):2433–2443.

Li, X., Jin, M., Zhou, N., Huang, J., Jiang, S., and Telesphore, H. (2016). Evaluation of evapotranspiration and deep percolation under mulched drip irrigation in an oasis of Tarim basin, China. *Journal of Hydrology*, 538:677–688.

Lohammar, A. T., Larsson, S., Linder, S., and Falk, S. O. (1980). FAST : Simulation Models of Gaseous Exchange in Scots Pine. *Ecological Bulletins*, (32):505–523.

Lu, H., Liu, T., Yang, Y., and Yao, D. (2014). A hybrid dual-source model of estimating evapotranspiration over different ecosystems and implications for satellite-based approaches. *Remote Sensing*, 6(9):8359–8386.

Lund, M. R. and Soegaard, H. (2003). Modelling of evaporation in a sparse millet crop using a two-source model including sensible heat advection within the canopy. *Journal of Hydrology*, 280(1-4):124–144.

Mahfouf, J. F. and Noilhan, J. (1991). Comparative-Study of Various Formulations of Evaporation From Bare Soil Using Insitu Data. *Journal of Applied Meteorology*, 30(9):1354–1365.

Mastrorilli, M., Katerji, N., Rana, G., and Nouna, B. B. (1998). Daily actual evapotranspiration measured with TDR technique in Mediterranean conditions. *Agricultural and Forest Meteorology*, 90(1-2):81–89.

Mata-González, R., McLendon, T., and Martin, D. W. (2005). The inappropriate use of crop transpiration coefficients (Kc) to estimate evapotranspiration in arid ecosystems: a review. *Arid Land Research and Management*, 19(3):285–295.

McCabe, M. F., Kalma, J. D., and Franks, S. W. (2005). Spatial and temporal patterns of land surface fluxes from remotely sensed surface temperatures within an uncertainty modelling framework. *Hydrology and Earth System Sciences*, 9(5):467–480.

McCuen, R. H. (1974). A sensitivity and error analysis of procedures used for estimating evaporation. *Journal of the American Water Resources Association*, 10:486–497.

Meijninger, W. M. L., Green, A. E., Hartogensis, O. K., Kohsiek, W., Hoedjes, J. C. B., Zuurbier, R. M., and De Bruin, H. A. R. (2002). Determination of area-averaged water vapour fluxes with large aperture and radio wave scintillometers over a heterogeneous surface - Flevoland field experiment. *Boundary-Layer Meteorology*, 105(1):63–83.

Merlin, O., Stefan, V. G., Amazirh, A., Chanzy, A., Ceschia, E., Er-Raki, S., Gentine, P., Tallec, T., Ezzahar, J., Bircher, S., Beringer, J., and Khabba, S. (2016). Modeling soil evaporation efficiency in a range of soil and atmospheric conditions using a meta-analysis approach. *Water Resources Research*, 52(5):3663 – 3684.

Misson, L., Panek, J. a., and Goldstein, A. H. (2004). A comparison of three approaches to modeling leaf gas exchange in annually drought-stressed ponderosa pine forests. *Tree physiology*, 24:529–541.

Monteith, J. (1995). A reinterpretation of stomatal responses to humidity. *Plant, Cell & Environment*, (1991):357–364.

Monteith, J. and Unsworth, M. (2013). *Principles of Environmental Physics - Plants, Animals, and the Atmosphere.* Elsevier Academic Press.

Monteith, J. L. (1965). Evaporation and environment. *Symposia of the Society for Experimental Biology*, 19:205–234.

Moreira, M., Sternberg, L., Martinelli, L., Victoria, R., Barbosa, E., Bonates, L., and Nepstad, D. (1997). Contribution of transpiration to forest ambient vapour based on isotopic measurements. *Global Change Biology*, 3(5):439–450.

Morton, F. I. (1994). Evaporation researcha critical review and its lessons for the environmental sciences. *Critical Reviews in Environmental Science and Technology*, 24(3):237 – 280.

Mu, Q., Zhao, M., and Running, S. W. (2011). Improvements to a MODIS global terrestrial evapotranspiration algorithm. *Remote Sensing of Environment*, 115(8):1781–1800.

Musgrave, R. B. and Moss, D. N. (1961). Photosynthesis under field conditions. I . A portable, closed system for determining net assimilation and respiration of corn. *Crop Science*, 1:37–41.

Nemani, R. R. and Running, S. W. (1989). Estimation of regional surface resistance to evapotranspiration from NDVI and thermal-IR AVHRR data.

Noe, S. M. and Giersch, C. (2004). A simple dynamic model of photosynthesis in oak leaves: coupling leaf conductance and photosynthetic carbon fixation by a variable intracellular CO2 pool. *Functional Plant Biology*, 31:1195–1204.

Noilhan, J. and Planton, S. (1989). A Simple Parameterization of Land Surface Processes for Meteorological Models.

Norman, J. M., Kustas, W. P., Prueger, J. H., and Diak, G. R. (2000). Surface flux estimation using radiometric temperature: A dual- temperature-difference method to minimize measurement errors. *Water Resources*, 36(8):2263–2274.

Oren, R., Sperry, J., Katul, G., Pataki, D., Ewers, B., Phillips, N., and Schäfer, K. (1999). Survey and synthesis of intra-and interspecific variation in stomatal sensitivity to vapour pressure deficit. *Plant, Cell & Environment*, 22(12):1515–1526.

Oudin, L., Hervieu, F., Michel, C., Perrin, C., Andréassian, V., Anctil, F., and Loumagne, C. (2005). Which potential evapotranspiration input for a lumped rainfall-runoff model? Part 2 - Towards a simple and efficient potential evapotranspiration model for rainfall-runoff modelling. *Journal of Hydrology*, 303(1-4):290–306.

Penman, H. L. (1948). Natural evaporation from open water, bare soil and grass. In *Proceedings of the Royal Society of London A: Mathematical, Physical and Engineering Sciences*, volume 193, pages 120–145. The Royal Society.

Priestley, C. H. B. and Taylor, R. J. (1972). On the assessment of surface heat flux and evaporation using large-scale parameters. *Monthly weather review*, 100(2):81–92.

Prueger, J., Hipps, L., and Cooper, D. (1996). Evaporation and the development of the local boundary layer over an irrigated surface in an arid region. *Agricultural and Forest Meteorology*, 78:223–237.

Rana, G. and Katerji, N. (1998). A measurement based sensitivity analysis of the Penman-Monteith actual evapotranspiration model for crops of different height and in contrasting water status. *Theoretical and Applied Climatology*, 60(1-4):141–149.

Rana, G. and Katerji, N. (2000). Measurement and estimation of actual evapotranspiration in the field under Mediterranean climate: A review. *European Journal of Agronomy*, 13(2-3):125–153.

Rana, G., Katerji, N., Mastrorilli, M., and Moujabber, M. E. (1997). A Model for Predicting Actual Evapotranspiration under Soil Water Stress in a Mediterranean Region. *Theoretical and Applied Climatology*, 56:45 – 55.

Raz-Yaseef, N., Rotenberg, E., and Yakir, D. (2010). Effects of spatial variations in soil evaporation caused by tree shading on water flux partitioning in a semi-arid pine forest. *Agricultural and Forest Meteorology*, 150(3):454–462.

Raz-Yaseef, N., Yakir, D., Schiller, G., and Cohen, S. (2012). Dynamics of evapotranspiration partitioning in a semi-arid forest as affected by temporal rainfall patterns. *Agricultural and Forest Meteorology*, 157:77–85.

Reicosky, D. C., Sharratt, B. S., Ljungkull, J. E., and Baker, D. G. (1983). Comparison of alfalfa evapotranspiration measured by a weighing lysimeter and a portable chamber. *Agricultural Meteorology*, 28:205–211.

Roerink, G. J., Su, Z., and Menenti, M. (2000). S-SEBI: A simple remote sensing algorithm to estimate the surface energy balance. *Physics and Chemistry of the Earth, Part B: Hydrology, Oceans and Atmosphere*, 25(2):147–157.

Romanenko, V. A. (1961). Computation of the autumn soil moisture using a universal relationship for a large area. *Proceedings Ukrainian Hydrometeorological Research Institute*, 3.

Rutter, A. J., Kershaw, K. A., Robins, P. C., and Morton, A. J. (1971). A predictive model of rainfall interception in forests, 1. Derivation of the model from observations in a plantation of Corsican pine. *Agricultural Meteorology*, 9(C):367–384.

Saxton, K. E. (1975). Sensitivity analyses of the combination evapotranspiration equation. *Agricultural Meteorology*, 15(3):343–353.

Schymanski, S. J. and Or, D. (2016). Leaf-scale experiments reveal important omission in the Penman-Monteith equation. *Hydrology and Earth System Sciences Discussions*, (July):1–33.

Seiller, G. and Anctil, F. (2016). How do potential evapotranspiration formulas influence hydrological projections? *Hydrological Sciences Journal*.

Sellers, P. J., Heiser, M. D., and Hall, F. G. (1992). Relations between surface conductance and spectral vegetation indices at intermediate (100 m sq to 15 km sq) length scales. *Journal of Geophysical Research*, 97(D17):19033–19959.

Shadmani, M., Marofi, S., and Roknian, M. (2012). Trend Analysis in Reference Evapotranspiration Using Mann-Kendall and Spearman's Rho Tests in Arid Regions of Iran. *Water Resources Management*, 26(1):211–224.

Shawcroft, R. W. and Gardner, H. R. (1983). Direct evaporation from soil under a row crop canopy. *Agricultural Meteorology*, 28(3):229–238.

Shuttleworth, W. J. (2006). Towards one-step estimation of crop water requirements. *Transactions of the American Academy of Agricultural and Biological Engineers*, 49(4):925–935.

Shuttleworth, W. J. (2007). Putting the "vap" into evaporation. *Hydrology and Earth System Sciences*, 11(1):210–244.

Shuttleworth, W. J. and Gurney, R. J. (1990). The theoretical relationship between foliage temperature and canopy resistance in sparse crops. *Quarterly Journal of the Royal Meteorological Society*, 116(492):497–519.

Shuttleworth, W. J. and Wallace, J. S. (1985). Evaporation from sparse crops-an energy combination theory. *Quarterly Journal of the Royal Meteorological Society*, 111(469):839–855.

Sill, B. L., Fowler, J. E., and Lagarenne Jr., W. R. (1984). Measurement of evaporation by a vapor budget technique. *Water Resources Research*, 20(1):147 – 152.

Singer, J. W., Heitman, J. L., Hernandez-Ramirez, G., Sauer, T. J., Prueger, J. H., and Hatfield, J. L. (2010). Contrasting methods for estimating evapotranspiration in soybean. *Agricultural Water Management*, 98(1):157–163.

Singh, V. P. and Xu, C.-Y. (1997). Evaluation and Generalization of 13 Mass-Transfer Equations for Determining Free Water Evaporation. *Hydrological Processes*, 11(3):311–323.

Soderberg, K., Good, S., Wang, L., and Caylor, K. (2012). Stable Isotopes of Water Vapor in the Vadose Zone: A Review of Measurement and Modeling Techniques. *Vadose Zone Journal*, 11(3):0.

Soegaard, H., Lund, M., and Bolwig, S. (1999). A comparison of modelled and measured millet production in northeastern Burkina Faso. *Geografisk Tidsskrift*, (SPEC. ISS. 2):69–80.

Sperry, J. S., Adler, F. R., Campbell, G. S., and Comstock, J. P. (1998). Limitation of plant water use by rhizosphere and xylem conductance: Results from a model. *Plant, Cell and Environment*, 21(4):347–359.

Stannard, D. I. (1993). Comparison of Penman-Monteith, Shuttleworth-Wallace, and Modified Priestley-Taylor Evapotranspiration Models for wildland vegetation in semiarid rangeland. *Water Resources Research*, 29(5):1379–1392.

Steduto, P., Katerji, N., Puertos-Molina, H., ??nl??, M., Mastrorilli, M., and Rana, G. (1997). Water-use efficiency of sweet sorghum under water stress conditions gas-exchange investigations at leaf and canopy scales. *Field Crops Research*, 54(2-3):221–234.

Stewart, J. B. (1988). Modelling surface conductance of pine forest. *Agricultural and Forest Meteorology*, 43(1):19–35.

Su, Z., Schmugge, T., Kustas, W. P., and Massman, W. J. (2001). An Evaluation of Two Models for Estimation of the Roughness Height for Heat Transfer between the Land Surface and the Atmosphere. *Journal of Applied Meteorology*, 40(11):1933–1951.

Tang, R., Li, Z. L., and Tang, B. (2010). An application of the Ts-VI triangle method with enhanced edges determination for evapotranspiration estimation from MODIS data in arid and semi-arid regions: Implementation and validation. *Remote Sensing of Environment*, 114(3):540–551.

Tardieu, F. and Davies, W. J. (1993). Integration of hydraulic and chemical signalling in the control of stomatal conductance and water status of droughted plants. *Plant, Cell & Environment*, 16(4):341–349.

Tenhunen, J. D., Sala Serra, A., Harley, P. C., Dougherty, R. L., and Reynolds, J. F. (1990). Factors influencing carbon fixation and water use by mediterranean sclerophyll shurbs during summer drought. *Oecologia.*, 82:381–393.

Thom, A. S. (1975). Momentum, mass and heat exchange of plant communities. *Vegetation and the Atmosphere*, 1:57 – 109.

Thompson, A., Gilley, J., and Norman, J. (1993). A sprinkler water droplet evaporation and plant canopy model: I. Model development. *Transactions of the ASAE*, 36(3):735–741.

Thornthwaite, C. W. (1948). An approach toward a rational classification of climate. *Geographical Review*, 38(1):55–94.

Tittebrand, A., Schwiebus, A., and Berger, F. H. (2005). The influence of land surface parameters on energy flux densities derived from remote sensing data. *Meteorologische Zeitschrift*, 14(2):227–236.

Tolk, J., Howell, T., Steiner, J., and Krieg, D. (1996). Corn canopy resistance determined from whole plant transpiration. In *Evapotranspiration and Irrigation Scheduling: Proceedings of the International Conference*, pages 347–351.

Tolk, J. A., Howell, T. A., Steiner, J. L., and Krieg, D. R. (1995). Aerodynamic characteristics of corn as determined by energy balance techniques.

Turc, L. (1961). Evaluation des besoins en eau d'irrigation, évapotranspiration potentielle. *Ann. agron*, 12(1):13 – 49.

Tyree, M. T. and Sperry, J. S. (1988). Do Woody-plants Operate Near the Point of Catastrophic Xylem Dysfunction Caused By Dynamic Water-stress - Answers From A Model. *Plant Physiology*, 88(3):574–580.

van Bavel, C. H. M. and Hillel, D. I. (1976). Calculating potential and actual evaporation from a bare soil surface by simulation of concurrent flow of water and heat. *Agricultural Meteorology*, 17(6):453–476.

Verma, S. B. (1989). Aerodynamic resistances to transfers of heat, mass and momentum. *Estimation of Areal Evapotranspiration*, 177(177):13–20.

Walker, G. K. (1983). Measurement of evaporation from soil beneath crop canopies. *Canadian Journal of Soil Science*, 63:137 – 141.

Ward, H. C., Evans, J. G., and Grimmond, C. S. B. (2015a). Infrared and millimetre-wave scintillometry in the suburban environment - Part 1: Structure parameters. *Atmospheric Measurement Techniques*, 8(3):1407–1424.

Ward, H. C., Evans, J. G., and Grimmond, C. S. B. (2015b). Infrared and millimetre-wave scintillometry in the suburban environment -Part 2: Large-area sensible and latent heat fluxes. *Atmospheric Measurement Techniques*, 8(3):1407–1424.

Wetzel, P. J., Atlas, D., and Eoodward, R. H. (1984). Determining soil moisture from geosynchronous satellite infrared data: A feasibility study.

Wetzel, P. J. and Chang, J.-T. (1987). Concerning the Relationship between Evapotranspiration and Soil Moisture. *Journal of Climate and Applied Meteorology*, 26(1):18–27.

White, D. A., Beadle, C. L., Sands, P. J., Worledge, D., and Honeysett, J. L. (1999). Quantifying the effect of cumulative water stress on stomatal conductance of Eucalyptus globulus and Eucalyptus nitens: a phenomenological approach. *Australian Journal of Plant Physiology*, 26(1):17 – 27.

Wilson, K. B., Hanson, P. J., Mulholland, P. J., Baldocchi, D. D., and Wullschleger, S. D. (2001). A comparison of methods for determining forest evapotranspiration and its components: Sap-flow, soil water budget, eddy covariance and catchment water balance. *Agricultural and Forest Meteorology*, 106(2):153–168.

Wu, H. (2016). Evapotranspiration estimation of Platycladus orientalis in Northern China based on various models. *Journal of Forestry Research*, 27(4):871–878.

Wullschleger, S. D., Meinzer, F. C., and Vertessy, R. A. (1998). A Review of Whole-Plant Water Use Studies in Tree. *Tree Physiology*, 18(8-9):499–512.

Xu, C. Y. and Singh, V. P. (2000). Evaluation and generalization of radiation-based methods for calculationg evaporation. *Hydrological Processes*, 14:339–349.

Xu, C. Y. and Singh, V. P. (2001). Evaluation and generalization of temperature-based methods for calculating evaporation. *Hydrological Processes*, 15(2):305–319.

Yang, S. and Tyree, M. (1994). Hydraulic architecture of Acer saccharum and A. rubrum: comparison of branches to whole trees and the contribution of leaves to hydraulic resistance. *Journal of Experimental Botany*, 45(271):179–186.

Yepez, E. A., Williams, D. G., Scott, R. L., and Lin, G. (2003). Partitioning overstory and understory evapotranspiration in a semiarid savanna woodland from the isotopic composition of water vapor. *Agricultural and Forest Meteorology*, 119(1-2):53–68.

Zhao, W., Liu, B., Chang, X., Yang, Q., Yang, Y., Liu, Z., Cleverly, J., and Eamus, D. (2016). Evapotranspiration partitioning, stomatal conductance, and components of the water balance: A special case of a desert ecosystem in China. *Journal of Hydrology*, 538:374–386.

Zheng, C., Wang, Q., and Li, P. (2016). Coupling SEBAL with a new radiation module and MODIS products for better estimation of evapotranspiration. *Hydrological Sciences Journal*, pages 1–13.

Zhou, M. C., Ishidaira, H., Hapuarachchi, H. P., Magome, J., Kiem, A. S., and Takeuchi, K. (2006). Estimating potential evapotranspiration using ShuttleworthWallace model and NOAA-AVHRR NDVI data to feed a distributed hydrological model over the Mekong River basin. *Journal of Hydrology*, 327:151–173.

Zhu, Z. Y., Chao, L. B. G., Wang, Z. Q., and Gao, R. Z. (2007). Study on diurnal variation of Populus evapotranspiration based on Shuttleworth-Wallace model (in Chinese). *Journal of Hydraulic Engineering*, 38(5):582 – 590.